Supporting information

For

Acetate-catalyzed hydroboration of CO_2 for the selective formation of methanol-equivalent products

Yuri C. A. Sokolovicz[a,b], David Specklin[a], Olalla Nieto Faza,[c] Béatrice Jacques,[a] Carlos Silva López,[c] João H. Z. dos Santos[b], Henri S. Schrekker[b,*], Samuel Dagorne[a,*]

[a]*Institute of Chemistry, Université de Strasbourg, CNRS, Strasbourg, France.*

[b]*Institute of Chemistry, Universidade Federal do Rio Grande do Sul, Porto Alegre, RS, Brazil.*

[c] *Depto. Química Orgánica, Universidade de Vigo, Facultade de Ciencias Campus As Lagoas, 32004, Ourense, Spain*

[*] Email: dagorne@unistra.fr, henri.schrekker@ufrgs.br

Table of Contents

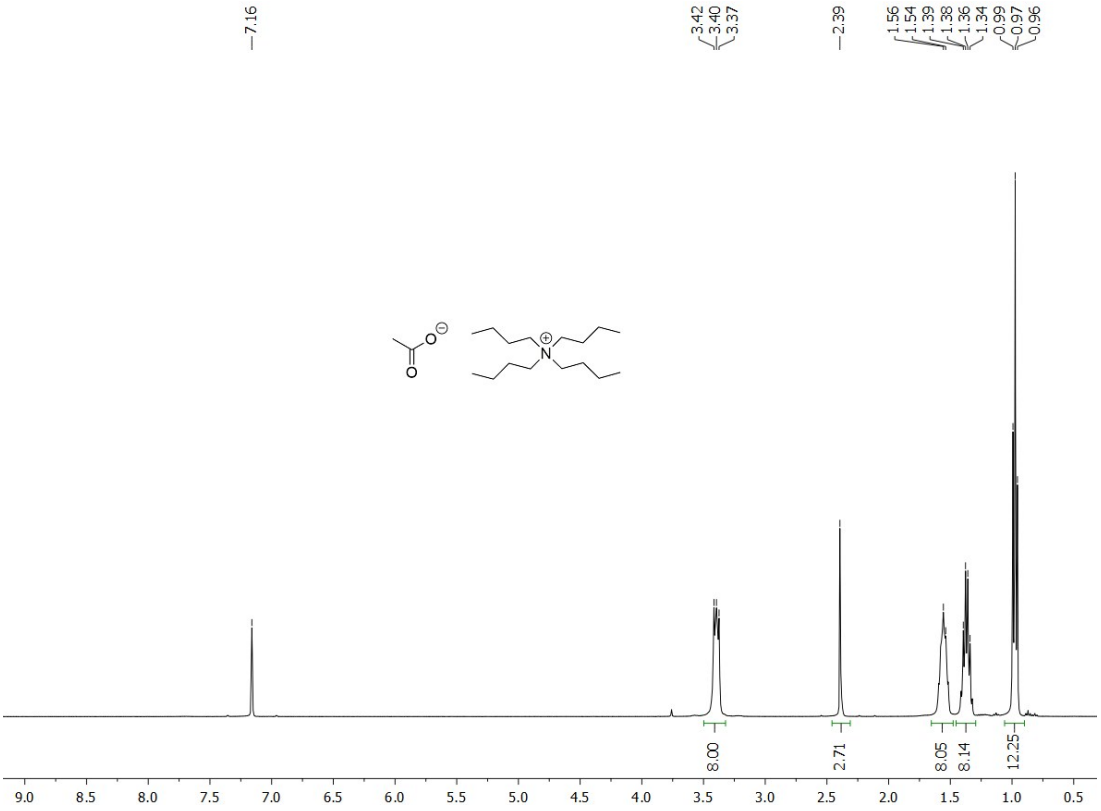

Figure S1. ^{1}H NMR spectrum (C_6D_6) of [TBA][OAc] (**1**).

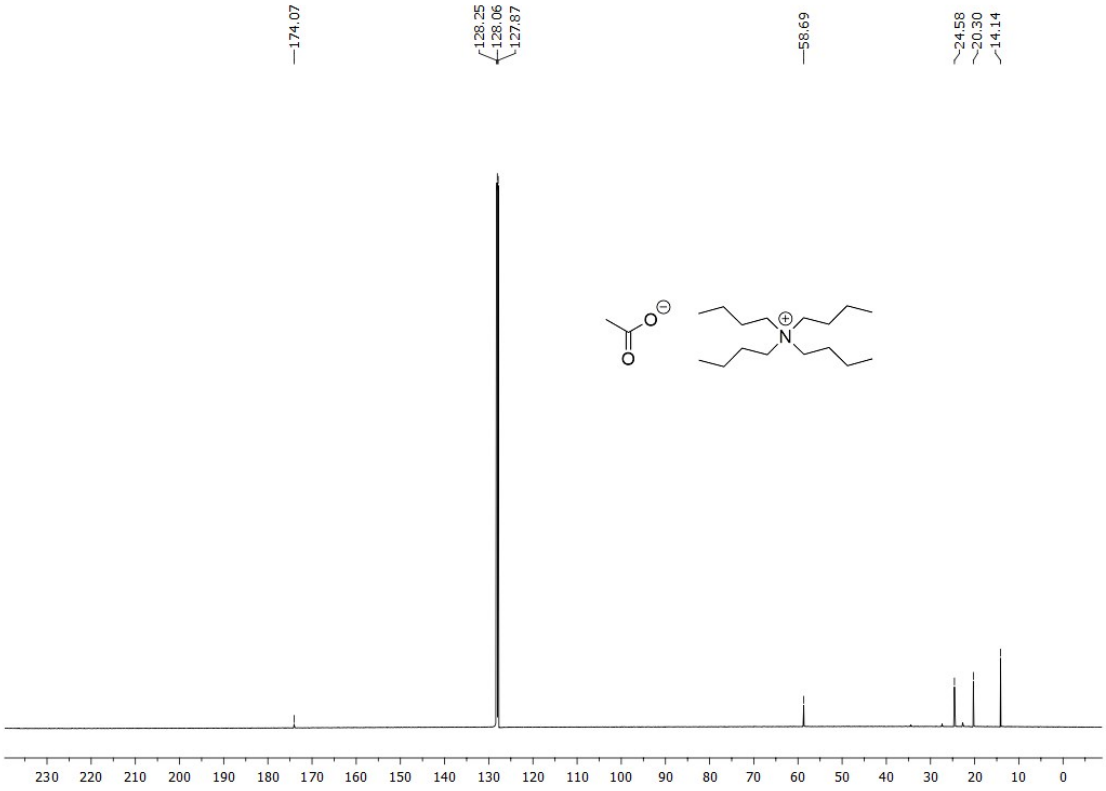

Figure S2. ^{13}C NMR spectrum (C_6D_6) of [TBA][OAc] (**1**).

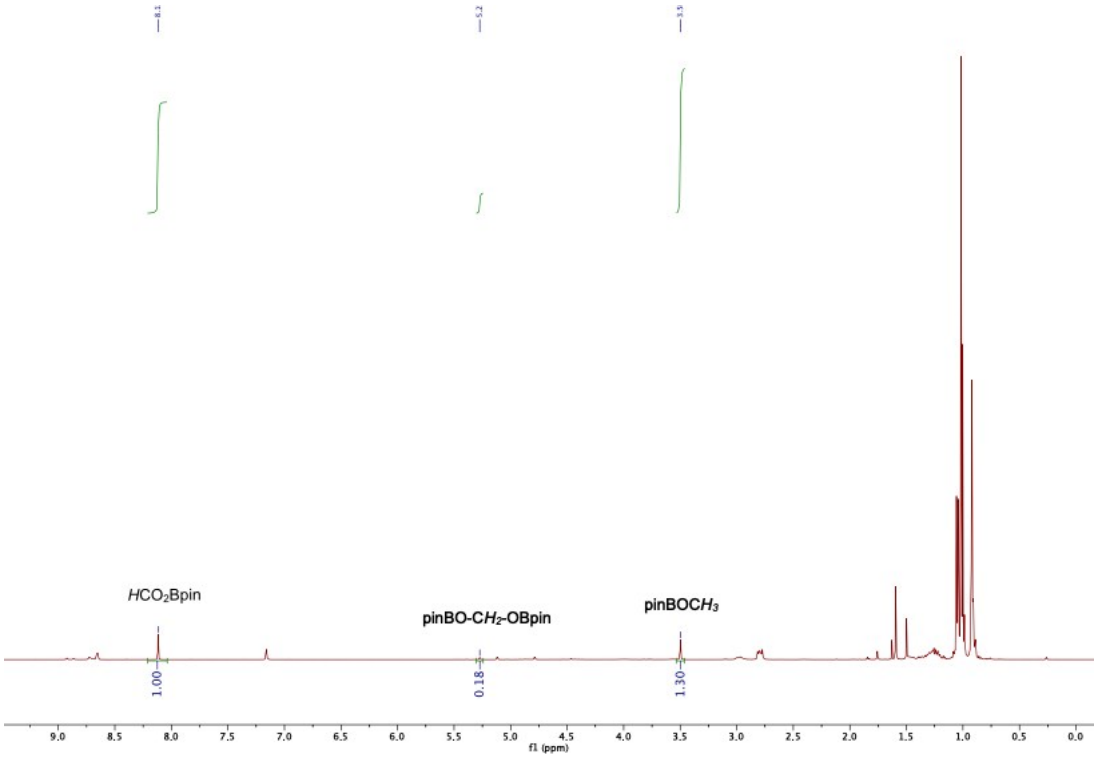

Figure S3. ^{1}H NMR spectrum after the reduction of CO_2 in the presence of HBpin and [TBA][OAc] (5 mol%). Conditions: C_6D_6; T = 90 °C; Time: 26 h; Borane conversion (82% conv) to a 11/1/4.7 $HCO_2Bpin/H_2C(OBpin)_2$/MeOBpin mixture. The residual C_6D_6 peak was used as an internal standard.

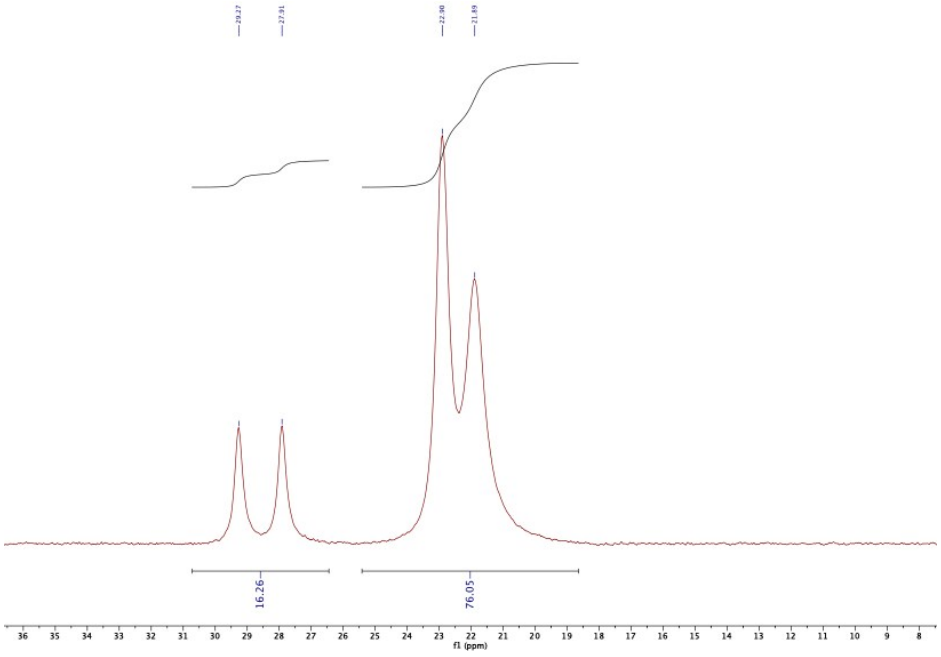

Figure S4. ^{11}B NMR spectrum after the reduction of CO_2 in the presence of HBpin and [TBA][OAc] (5 mol%). Conditions: C_6D_6; T = 90 °C; Time: 26 h; Borane conversion: 82%.

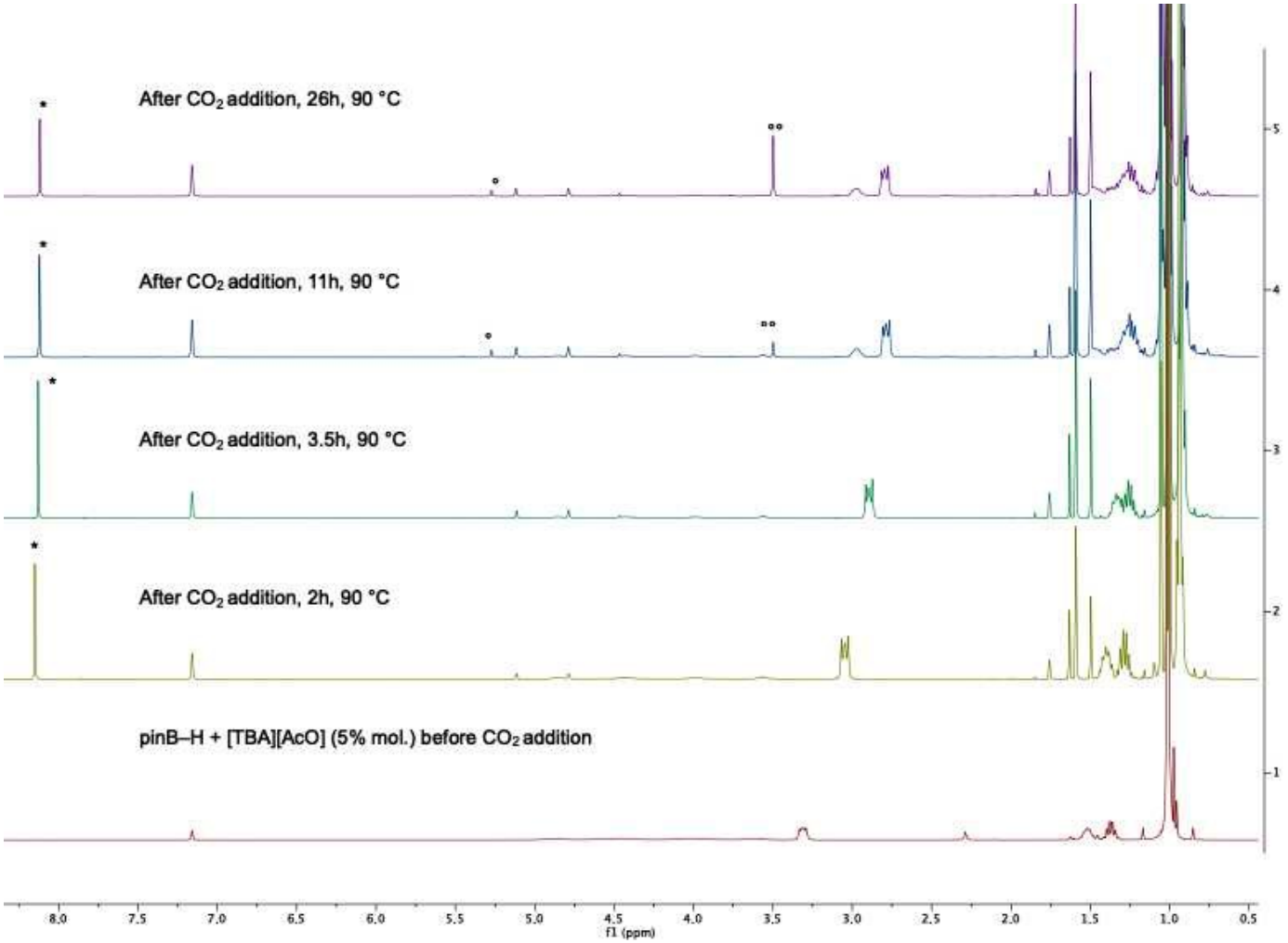

Figure S5. ^{1}H NMR monitoring data of the reduction of CO_2 in the presence of HBpin and [TBA][OAc] (5 mol%) as a function of time. Conditions: C_6D_6; T = 90 °C. The residual C_6D_6 peak was used as an internal standard. *: *H*CO_2Bpin; °: $H_2C(OBpin)_2$; °°: *Me*OBpin.

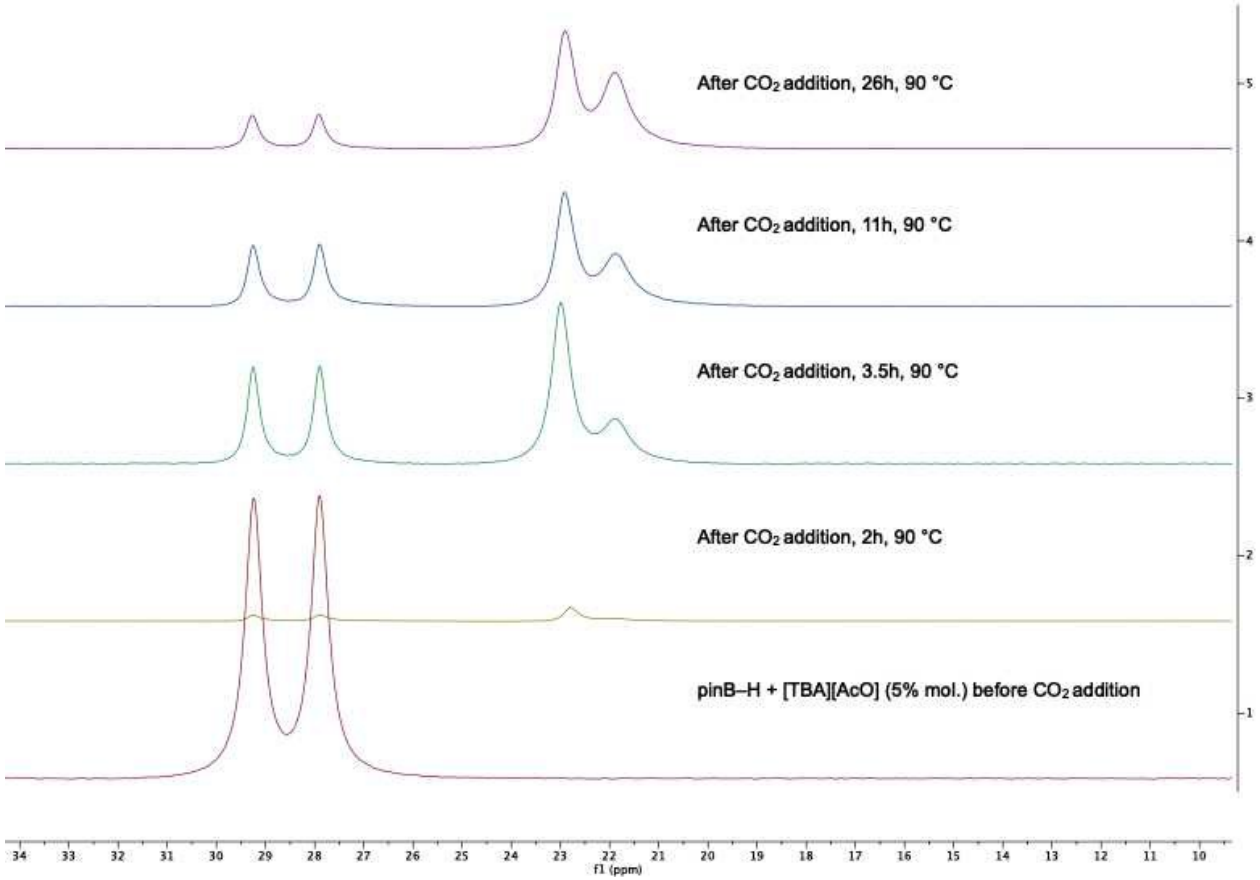

Figure S6. ^{11}B NMR monitoring data of the reduction of CO_2 in the presence of HBpin and [TBA][OAc] (5 mol%) as a function of time. Conditions: C_6D_6; T = 90 °C

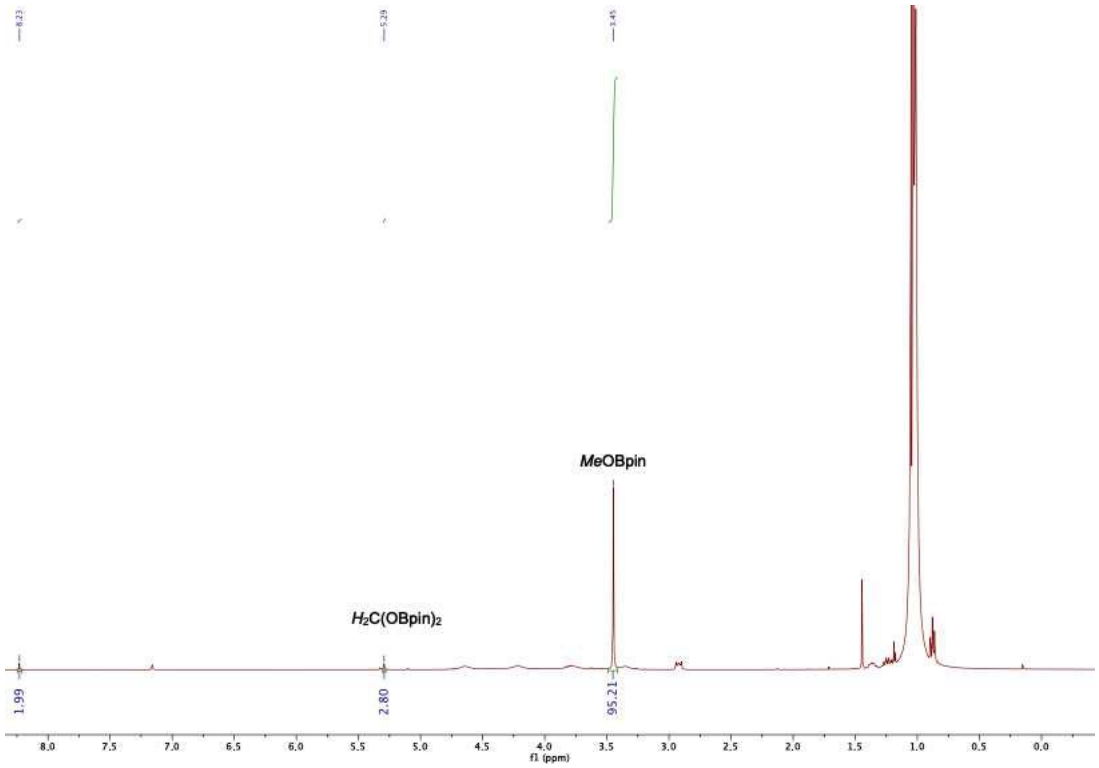

Figure S7. ^{1}H NMR spectrum after the reduction of CO_2 in the presence of HBpin and [TBA][OAc] (0.5 mol%). Conditions: C_6D_6; T: 90 °C; Time: 2 h; Borane conversion: 40%.

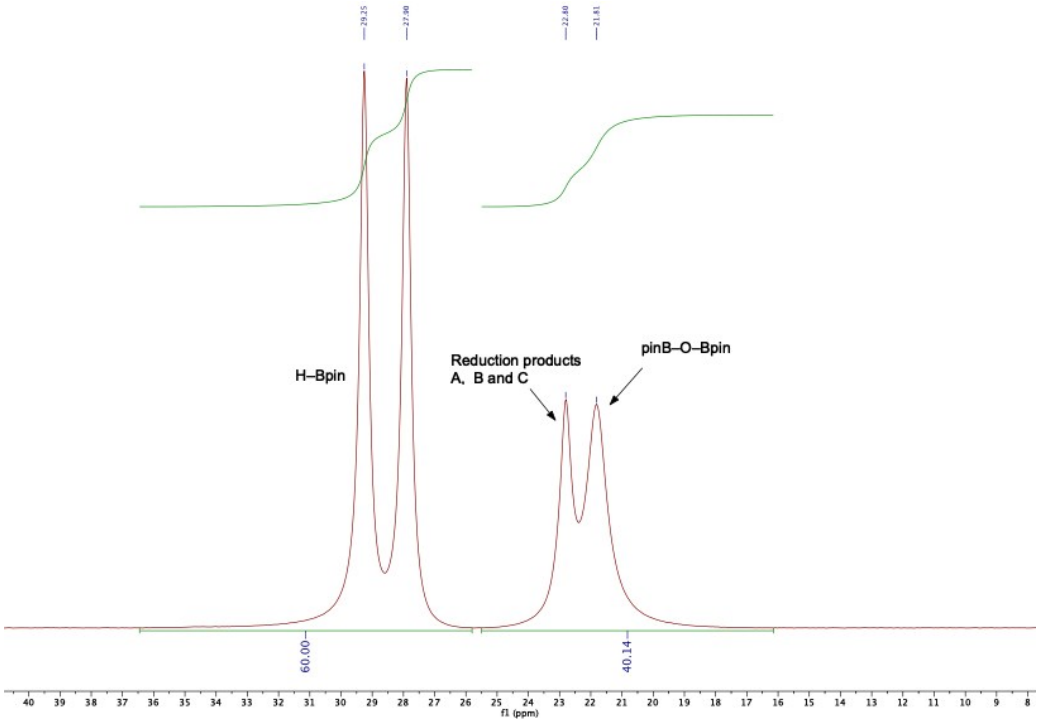

Figure S8. ^{11}B NMR spectrum after the reduction of CO_2 in the presence of HBpin and [TBA][OAc] (0.5 mol%). Conditions: C_6D_6; T: 90 °C; Time: 2 h; Borane conversion: 40%.

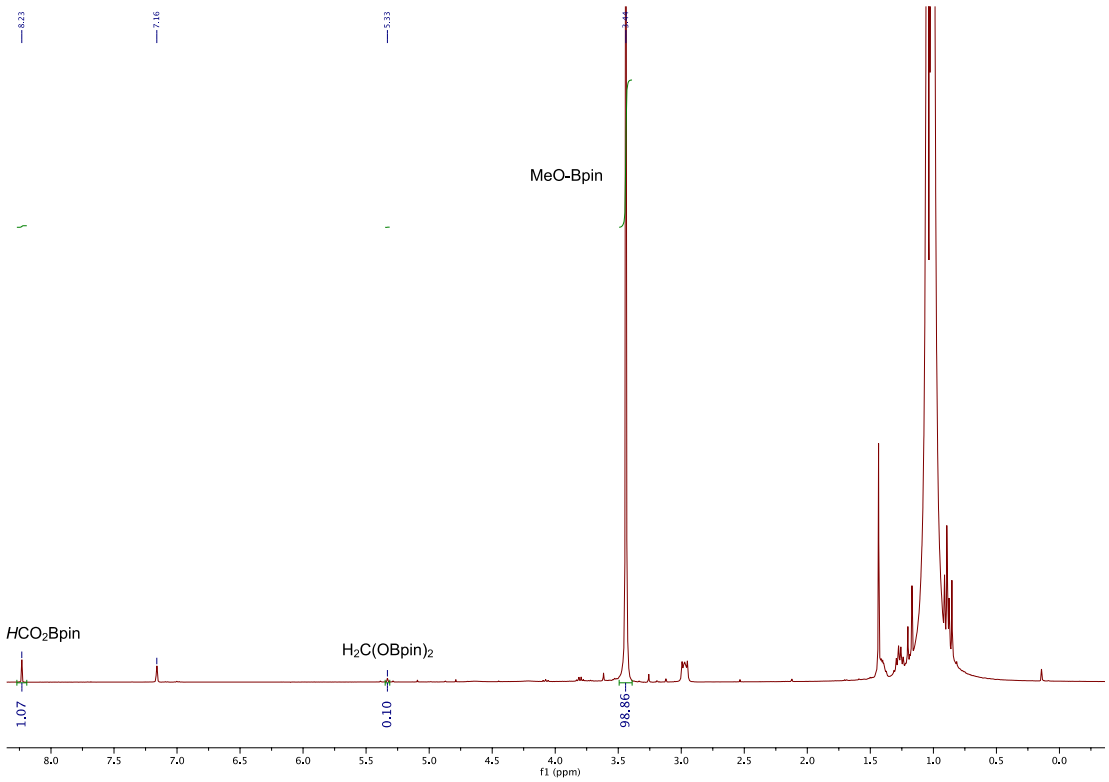

Figure S9. ^{1}H NMR spectrum after the reduction of CO_2 in the presence of HBpin and [TBA][OAc] (0.5 mol%). Conditions: C_6D_6; T: 90 °C; Time: 20 h; Borane conversion: 96 %.

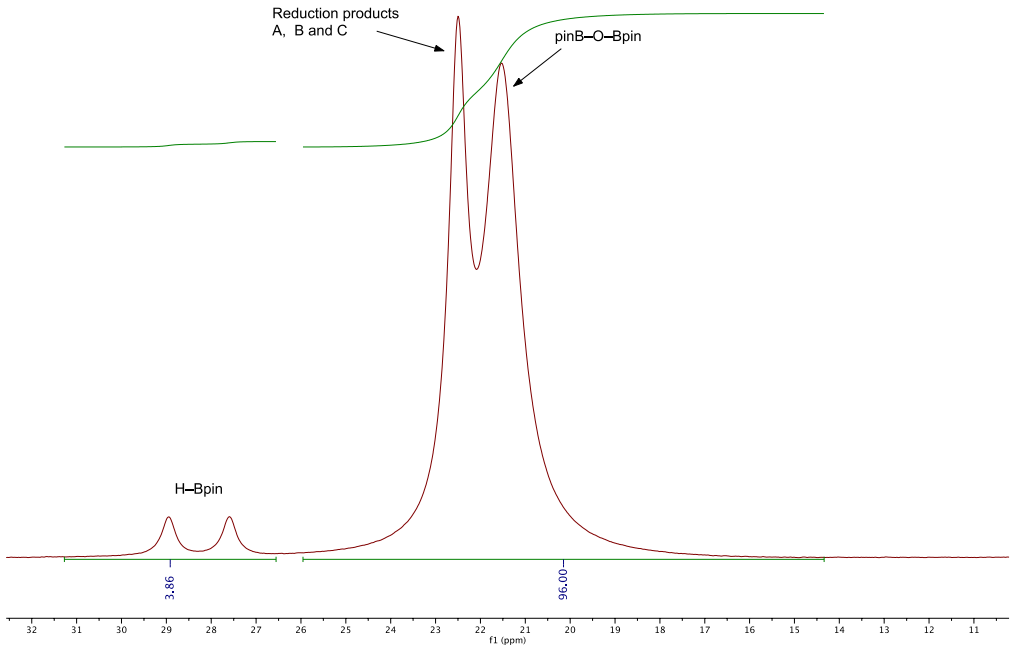

Figure S10. ^{11}B NMR spectrum after the reduction of CO_2 in the presence of HBpin and [TBA][OAc] (0.5 mol%). Conditions: C_6D_6; T: 90 °C; Time: 20 h; Borane conversion: 96 %. Compounds A, B and C correspond to hydroboration products HCO_2Bpin (**A**), $H_2C(OBpin)_2$ (**B**) and MeOBpin (**C**), respectively.

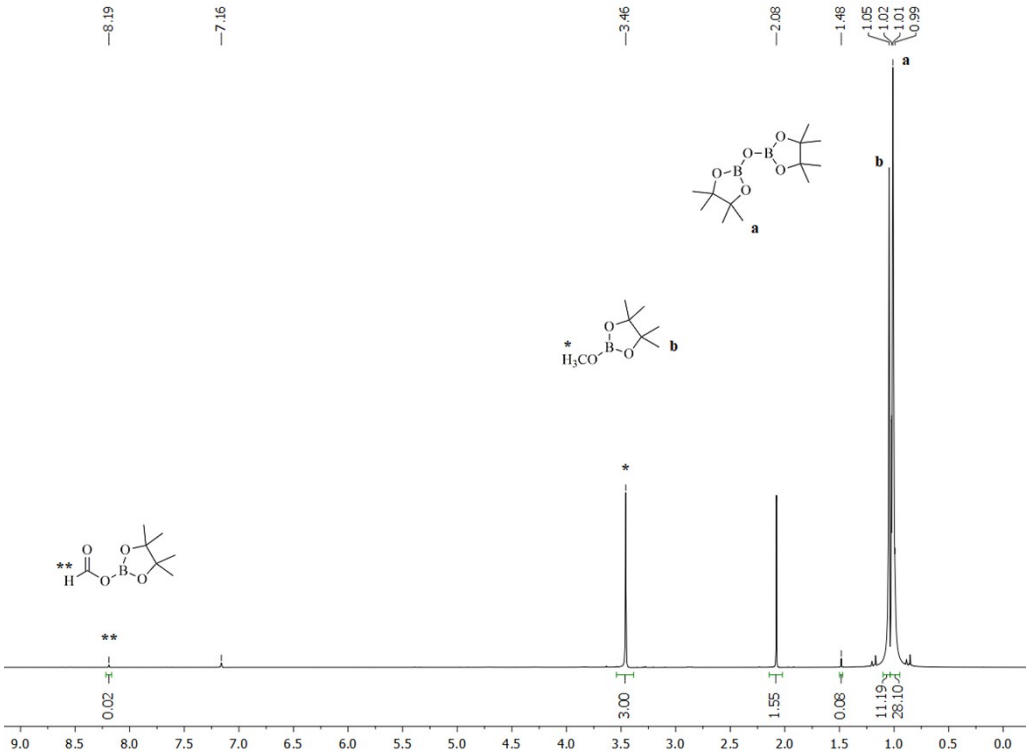

Figure S11. ^{1}H NMR spectrum after the reduction of CO_2 in the presence of HBpin and [TBA][OAc] (0.1 mol%). Conditions: C_6D_6, T = 90 °C, 20 h; Borane conversion: 94 %. Internal standard: hexamethylbenzene.

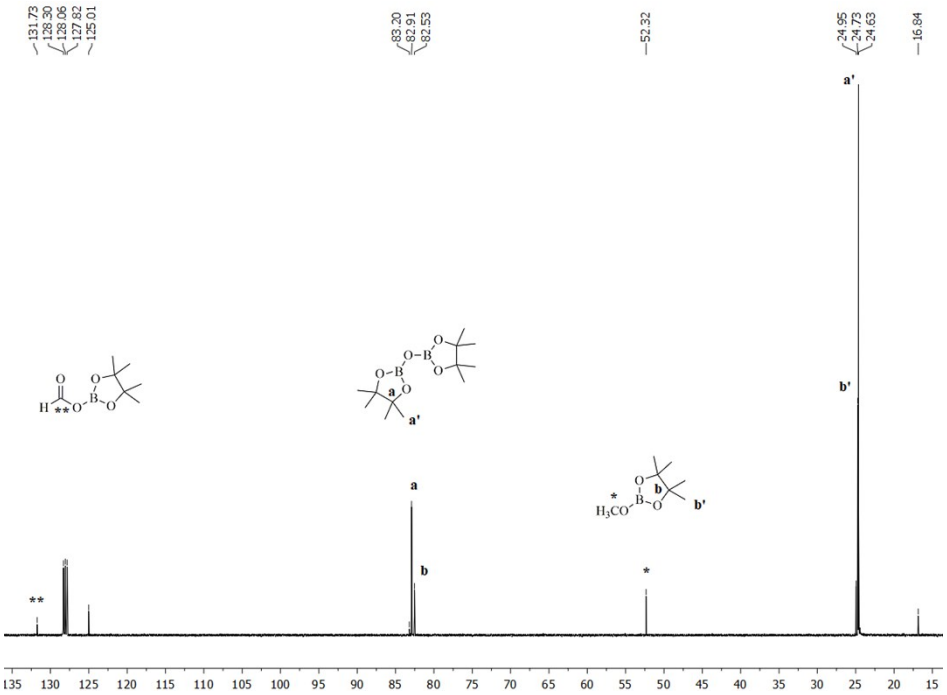

Figure S12. ^{13}C NMR spectrum after the reduction of CO_2 in the presence of HBpin and [TBA][OAc] (0.1 mol%). Conditions: C_6D_6, T = 90 ºC; 46 h; Borane conversion: 94%. Internal standard: hexamethylbenzene.

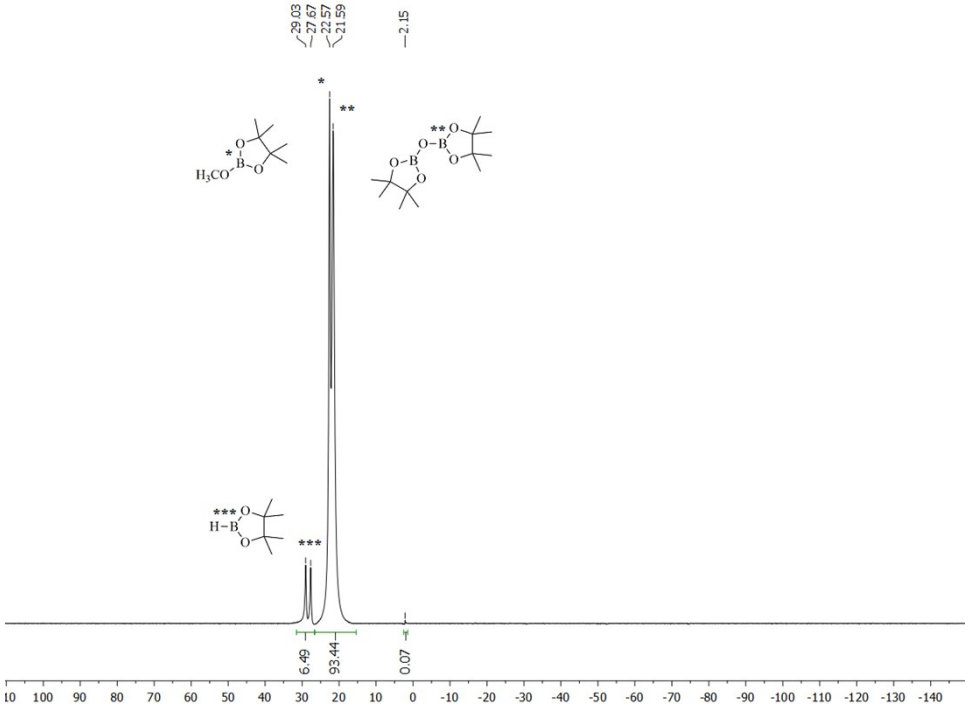

Figure S13. ^{11}B NMR spectrum after the reduction of CO_2 in the presence of HBpin and [TBA][OAc] (0.1 mol%). Conditions: C_6D_6, T = 90 ºC, 46 h; Borane conversion: 94%; Internal standard: hexamethylbenzene.

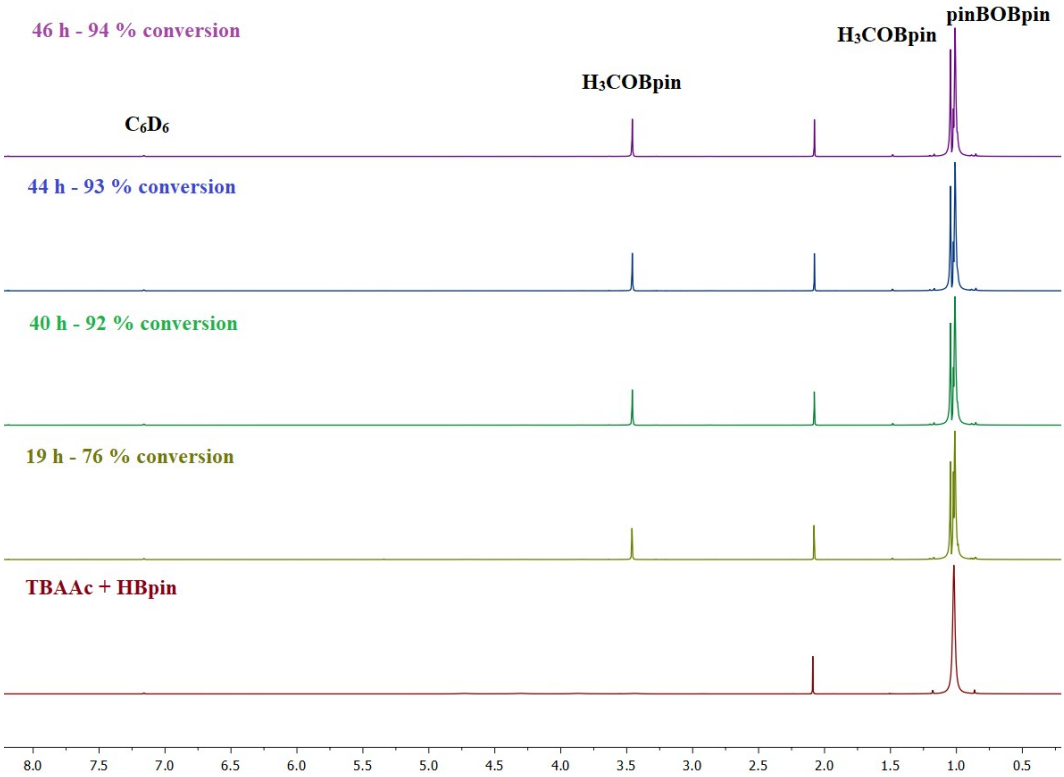

Figure S14. ^{1}H NMR monitoring spectra of the reduction of CO_2 in the presence of HBpin and [TBA][OAc] (0.1 mol%). Conditions: C_6D_6, T = 90 ºC. Internal standard: hexamethylbenzene.

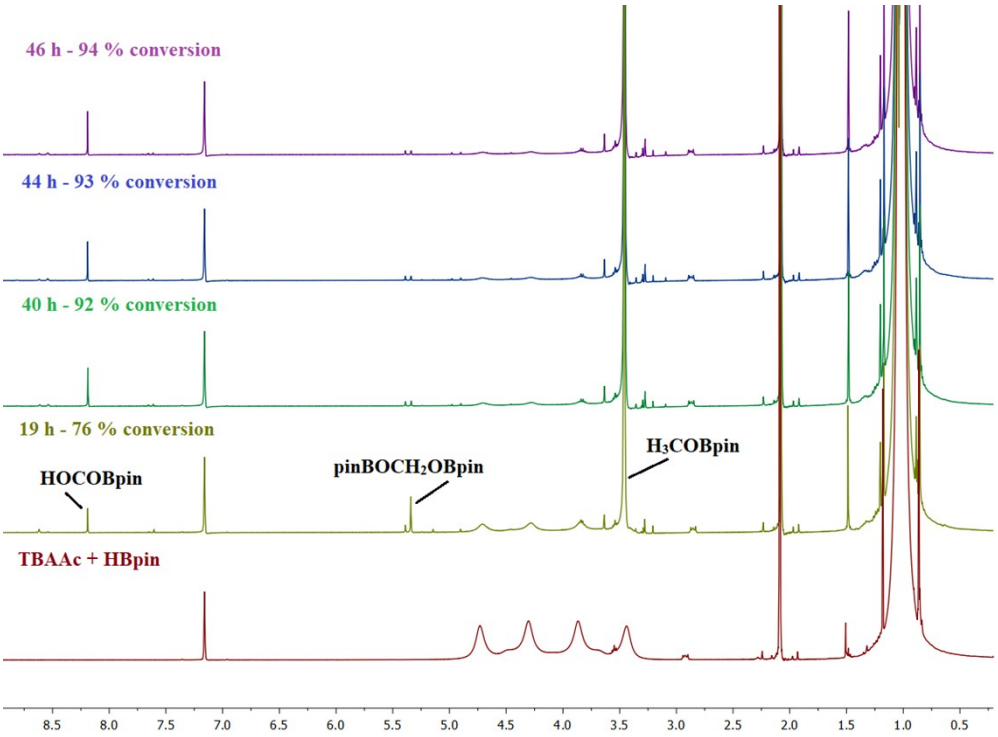

Figure S15. Blow-up of the ^{1}H NMR monitoring spectra of the reduction of CO_2 in the presence of HBpin and [TBA][OAc] (0.1 mol%). Conditions: C_6D_6, T = 90 ºC. Internal standard: hexamethylbenzene.

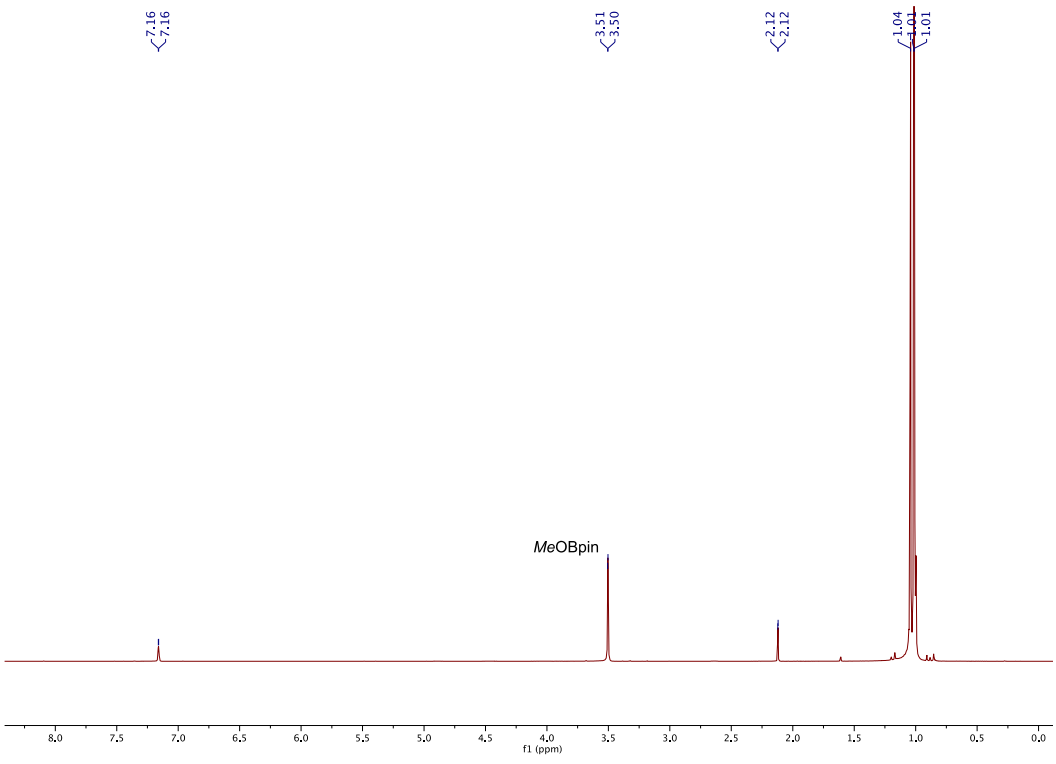

Figure S16. ^{1}H NMR spectrum of the reduction of CO_2 in the presence of HBpin and [TBA][OAc] (0.1 mol%) under solvent-free conditions after complete conversion to MeOBpin. Conditions: T = 90 ºC, 19 h. Internal standard: hexamethylbenzene.

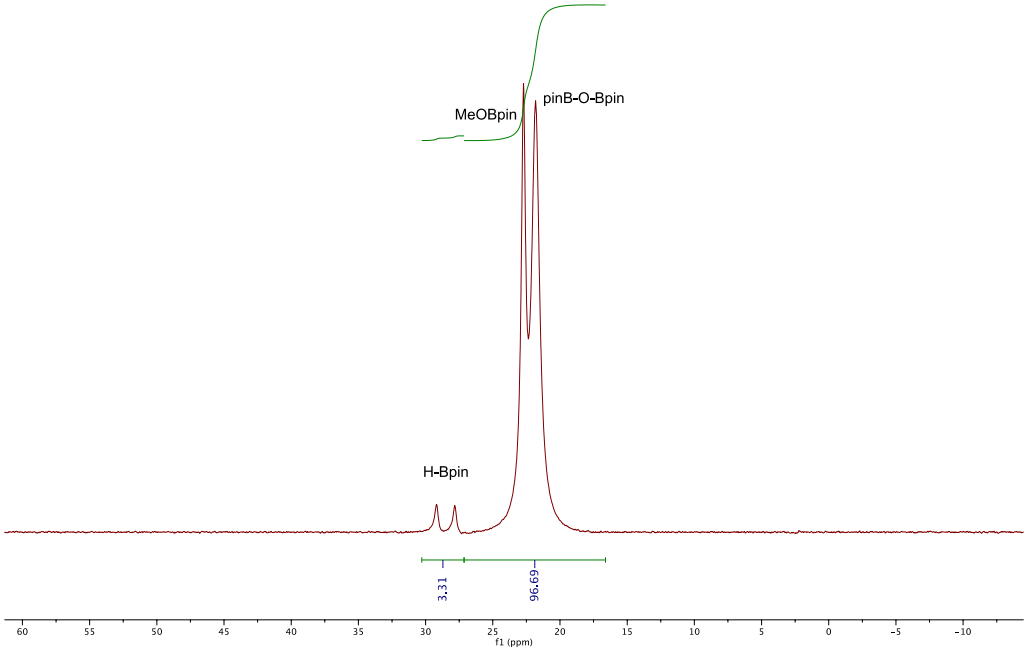

Figure S17. ^{11}B NMR spectrum of the reduction of CO_2 in the presence of HBpin and [TBA][OAc] (0.1 mol%) under solvent-free conditions after complete conversion to MeOBpin. Conditions: T = 90 ºC, 19 h. Internal standard: hexamethylbenzene.

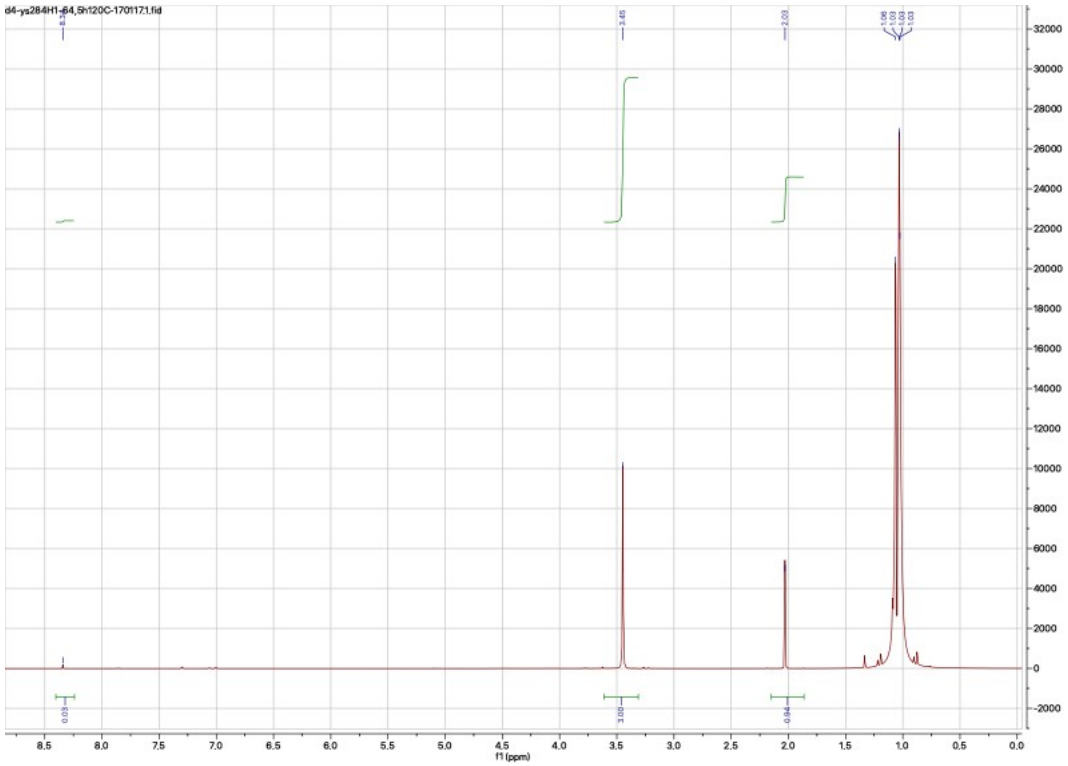

Figure S18. ^{1}H NMR spectrum of the reduction of CO_2 in the presence of HBpin and NaOAc (0.1 mol% *vs.* H-Bpin). Conditions: C_6D_5Br, 120 °C, 65 h, Borane conv: 96% (hexamethylbenzene, internal standard).

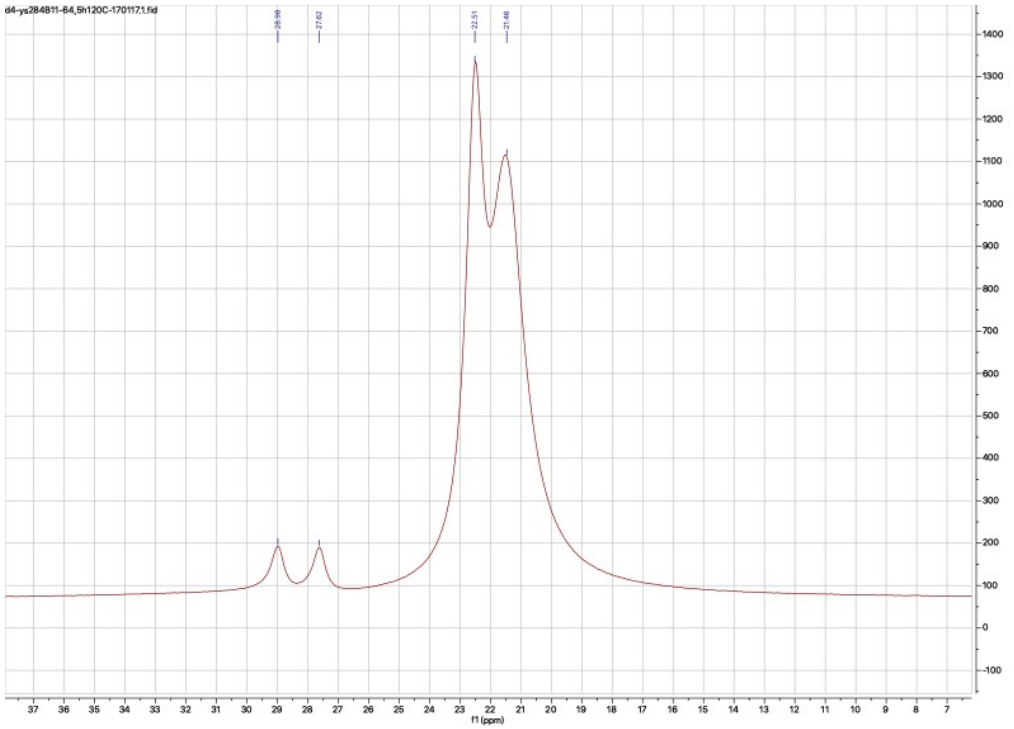

Figure S19. ^{11}B NMR spectrum of the reduction of CO_2 in the presence of HBpin and NaOAc (0.1 mol% *vs.* H-Bpin). Conditions: C_6D_5Br, 120 °C, 65 h. Borane conv: 96%.

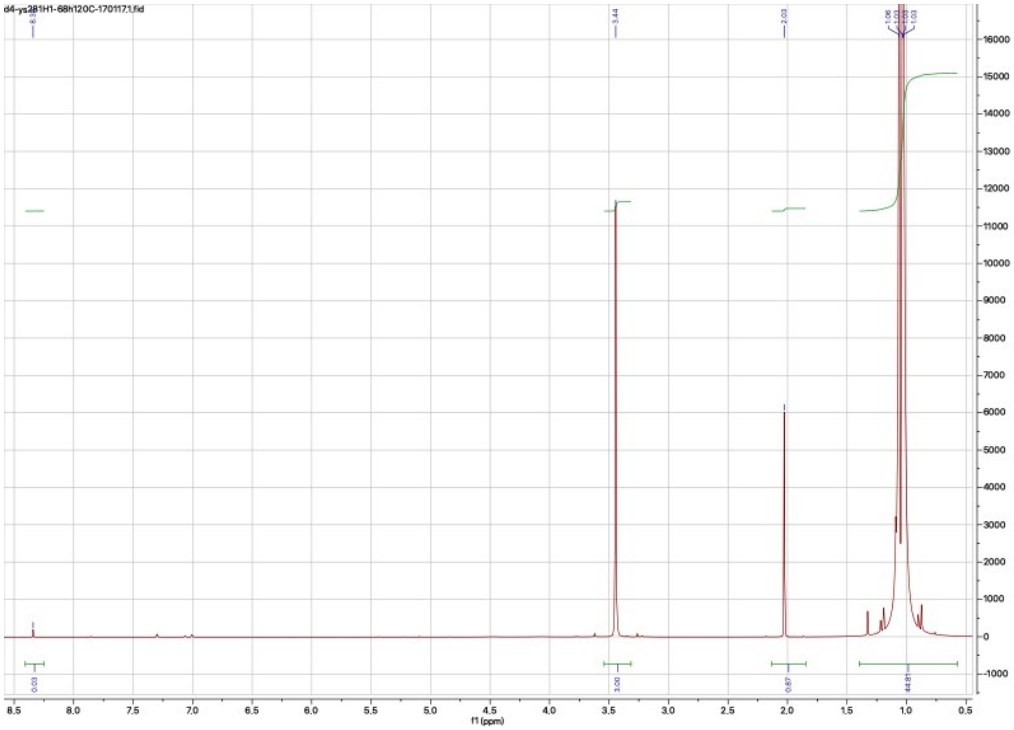

Figure S20. ^{1}H NMR spectrum of the reduction of CO_2 in the presence of HBpin and KOAc (0.1 mol% *vs.* H-Bpin). Conditions: C_6D_5Br, 120 °C, 65 h. Borane conversion: 94%. Internal standard: hexamethylbenzene.

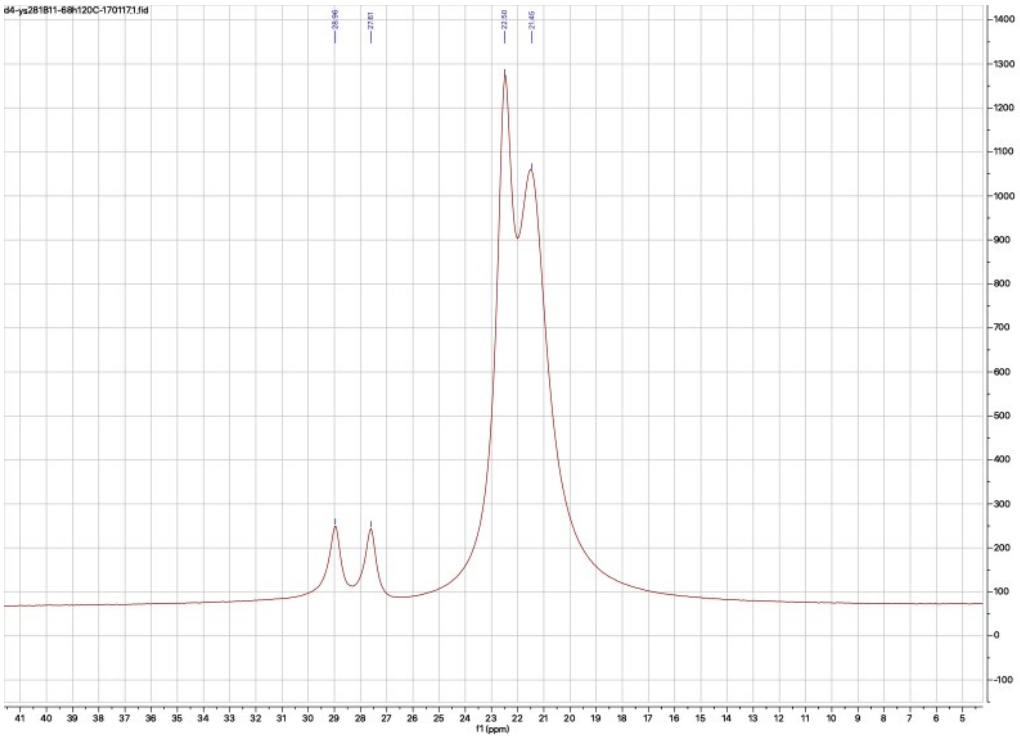

Figure S21. ^{11}B NMR spectrum of the reduction of CO_2 in the presence of HBpin and KOAc (0.1 mol% *vs.* H-Bpin). Conditions: C_6D_5Br, 120 °C, 65 h, 94% conversion to *Me*OBpin.

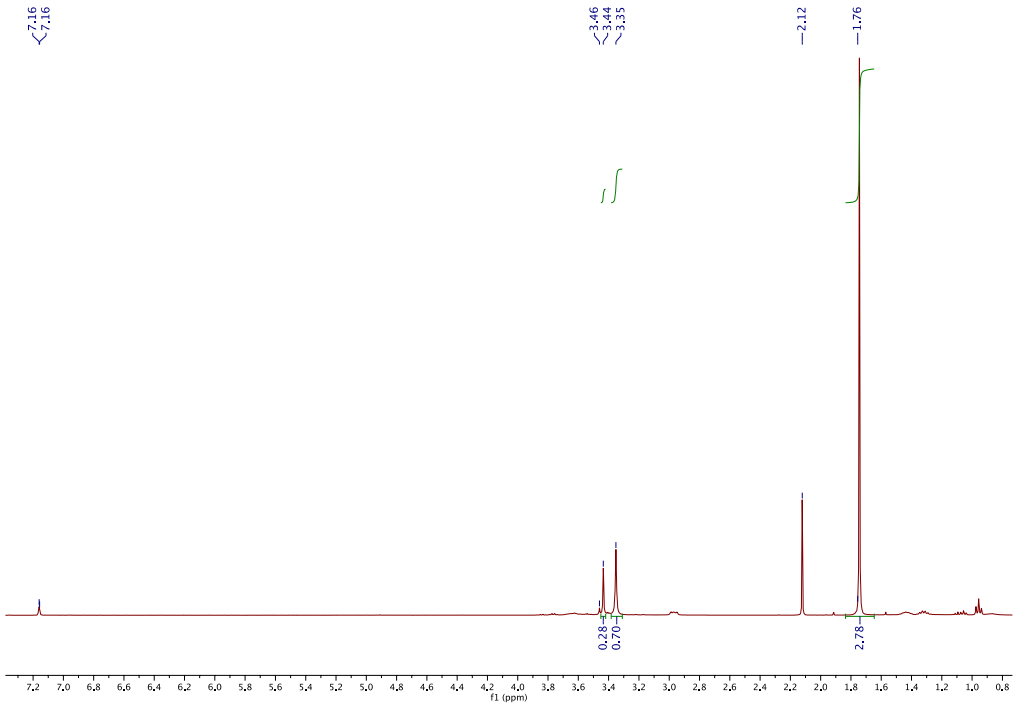

Figure S22. ^{1}H NMR spectrum of the reduction of CO_2 by H_3B-SMe_2 catalyzed by [TBA][OAc] (10 mol% *vs.* BH_3-SMe_2). Conditions: C_6D_6, RT, 17 h. C_6Me_6 (δ 2.12) was used as an internal standard. Quantitative conversion to a 70/30 $(MeOBO)_3$/$B(OMe)_3$ mixture.

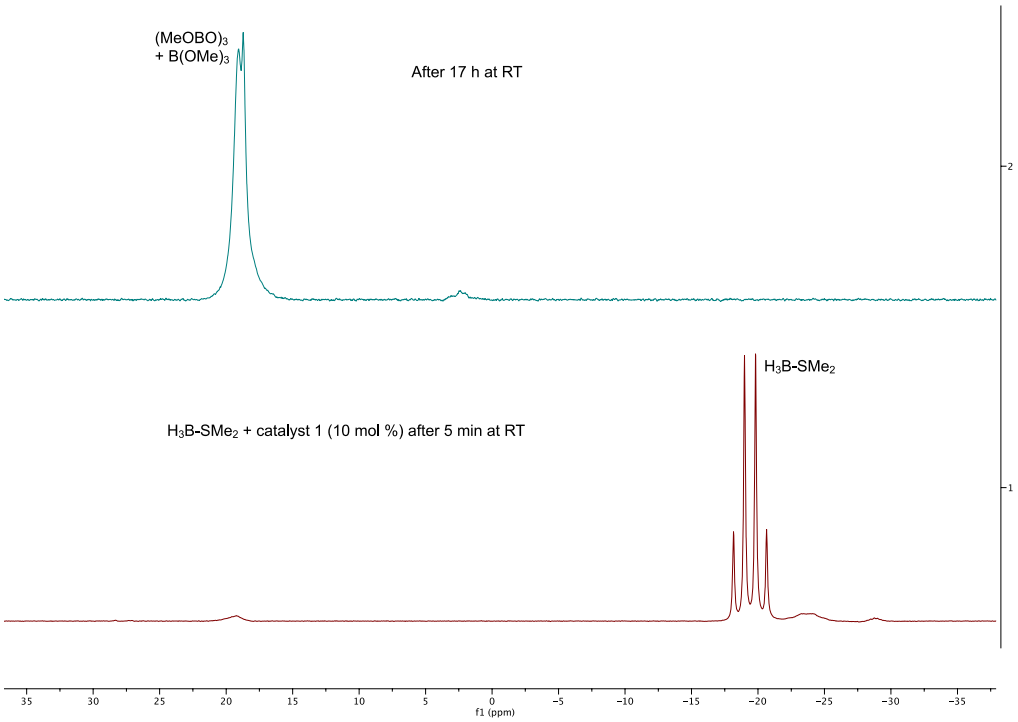

Figure S23. ^{11}B NMR spectrum of the reduction of CO_2 by H_3B-SMe_2 catalyzed by [TBA][OAc] (10 mol% *vs.* BH_3-SMe_2). Conditions: C_6D_6, RT, 17 h. C_6Me_6 was used as an internal standard. Quantitative borane conversion to a 70/30 $(MeOBO)_3/B(OMe)_3$ mixture.

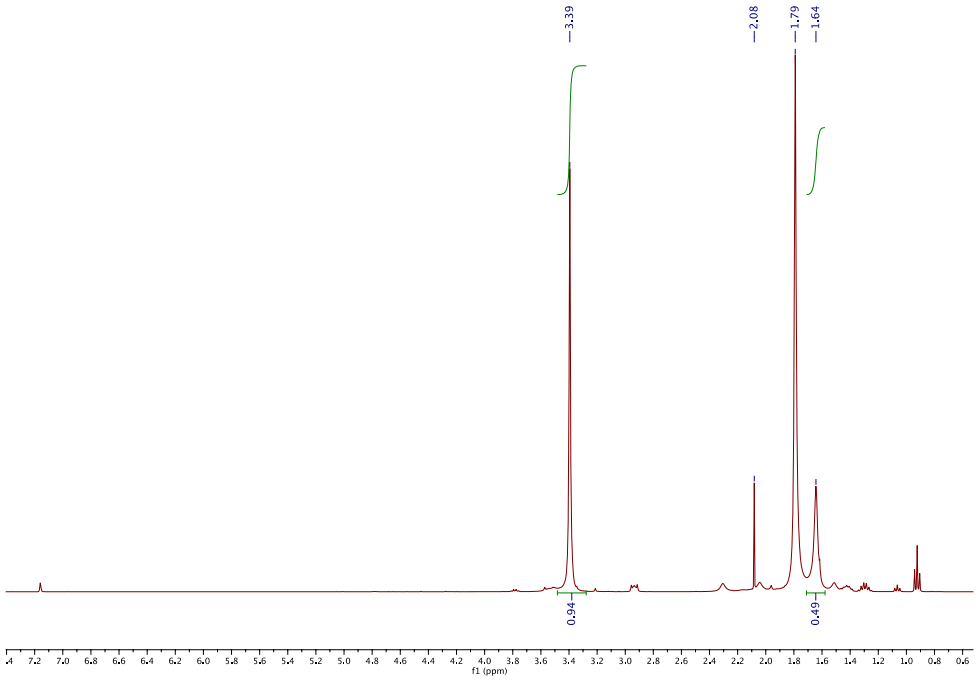

Figure S24. ^{1}H NMR spectrum of the reduction of CO_2 by H_3B-SMe_2 catalyzed by [TBA][OAc] (1 mol% *vs.* BH_3-SMe_2). Conditions: C_6D_6, RT, 48 h. C_6Me_6 was used as an internal standard. 68% borane conversion to reduction product $(MeOBO)_3$.

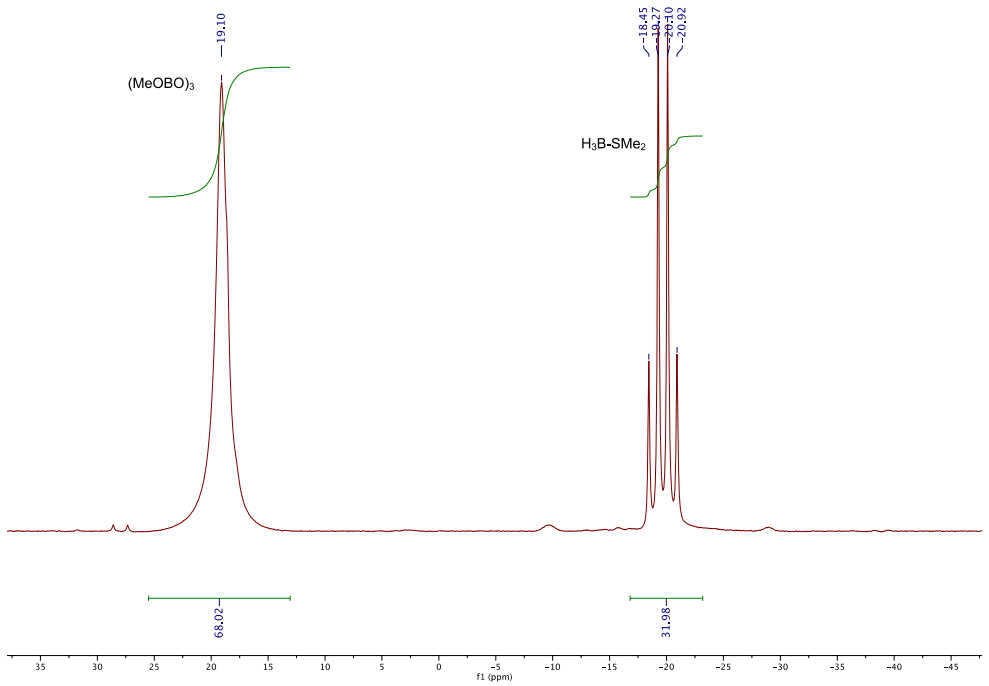

Figure S25. ^{11}B NMR spectrum of the reduction of CO_2 by H_3B-SMe_2 catalyzed by [TBA][OAc] (1 mol% *vs.* BH_3-SMe_2). Conditions: C_6D_6, RT, 48 h. 68% borane conversion to reduction product $(MeOBO)_3$.

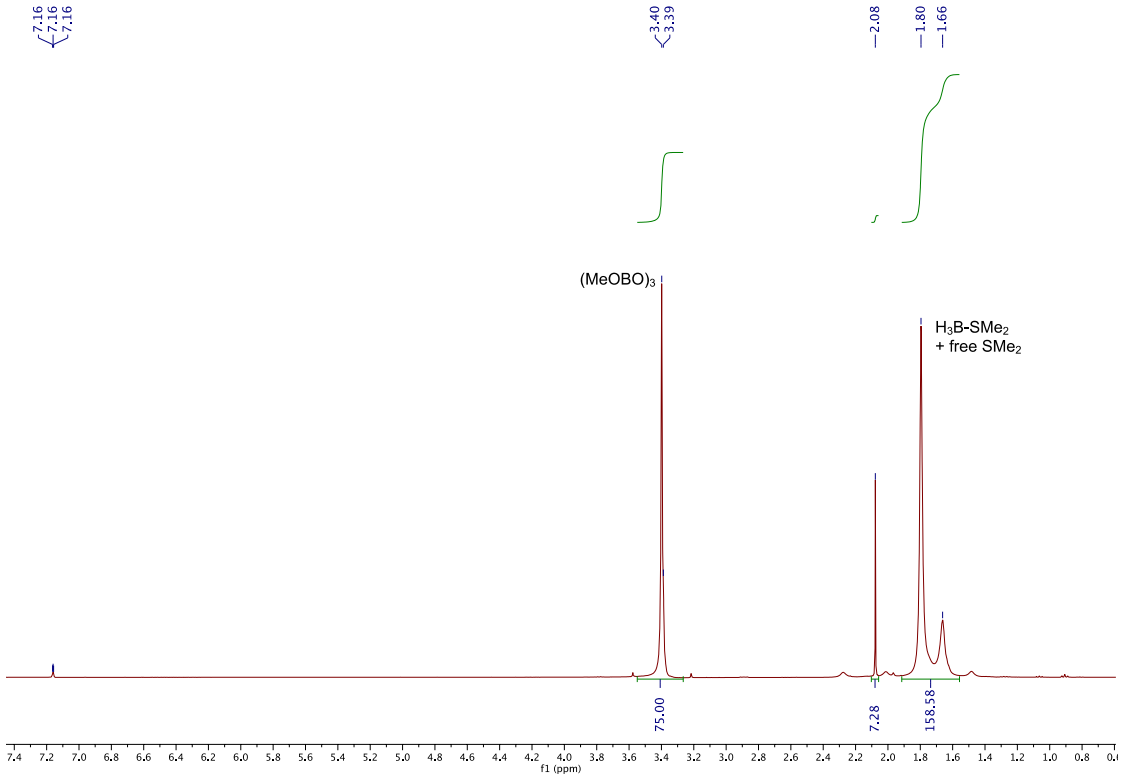

Figure S26. ^{1}H NMR spectrum of the reduction of CO_2 by H_3B-SMe_2 catalyzed by [TBA][OAc] (0.1 mol% *vs.* BH_3-SMe_2). Conditions: C_6D_6, 60 °C, 20 h. C_6Me_6 was used as an internal standard. 75 % borane conversion to reduction product $(MeOBO)_3$.

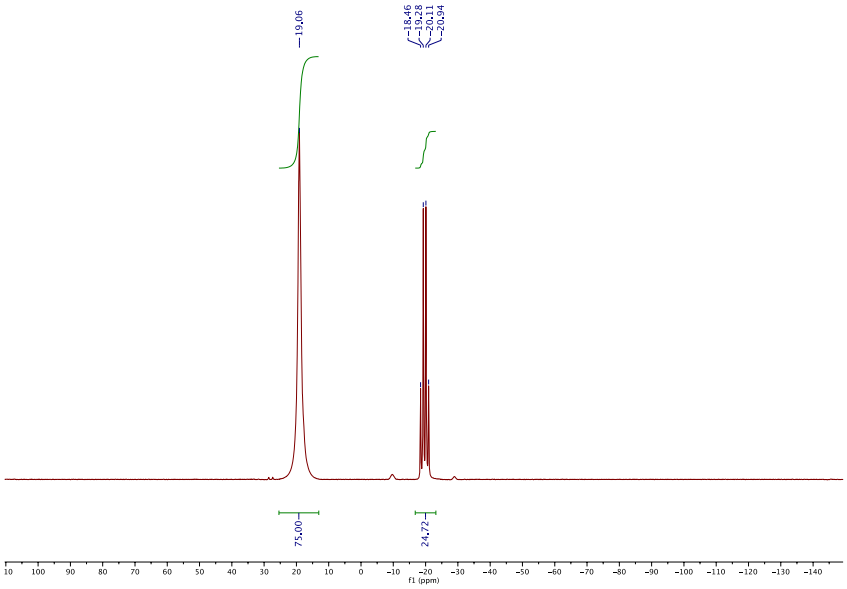

Figure S27. ^{11}B NMR spectrum of the reduction of CO_2 by H_3B-SMe_2 catalyzed by [TBA][OAc] (0.1 mol% *vs.* BH_3-SMe_2). Conditions: C_6D_6, 60 °C, 20 h. C_6Me_6 was used as an internal standard. 75 % borane conversion to reduction product $(MeOBO)_3$.

NMR data for stoichiometric monitoring reactions: 1/1 [TBA][OAc]/pinB–H; 1/1/1 [TBA][OAc]/pinB–H/CO_2 (1.5 atm)

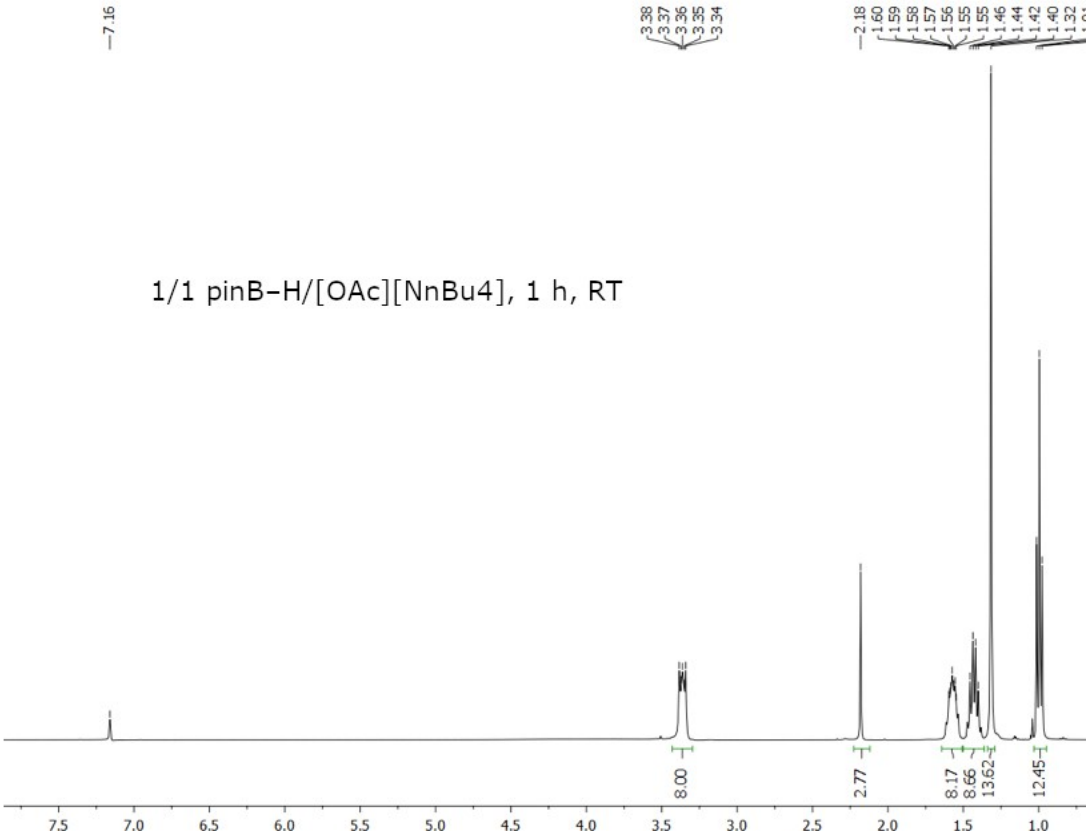

Figure S28. ^{1}H NMR spectrum (C_6D_6) of the stoichiometric reaction between [TBA][OAc] and HBpin after 1h at room temperature.

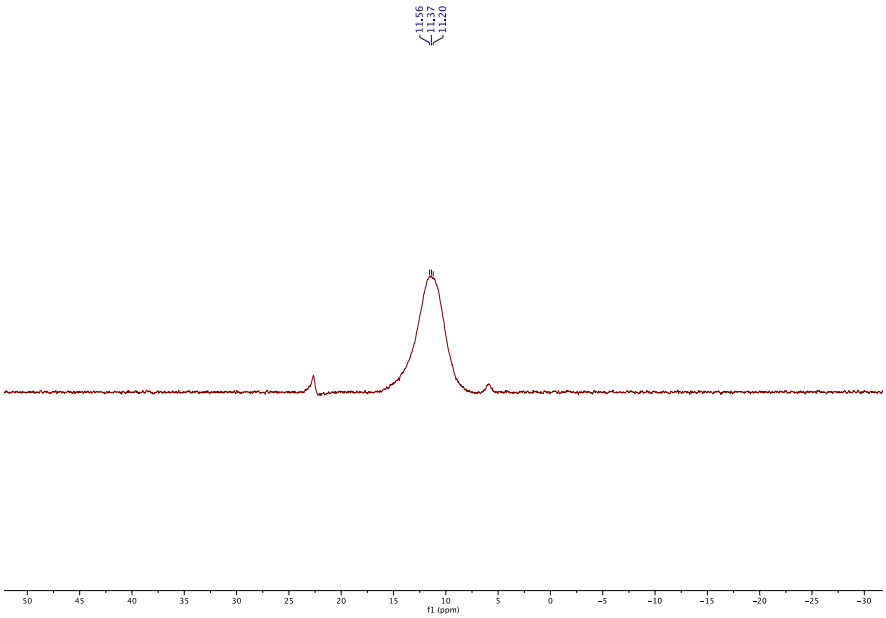

Figure S29. ^{11}B NMR spectrum (C_6D_6) of the stoichiometric reaction between [TBA][OAc] and HBpin (1 h, RT).

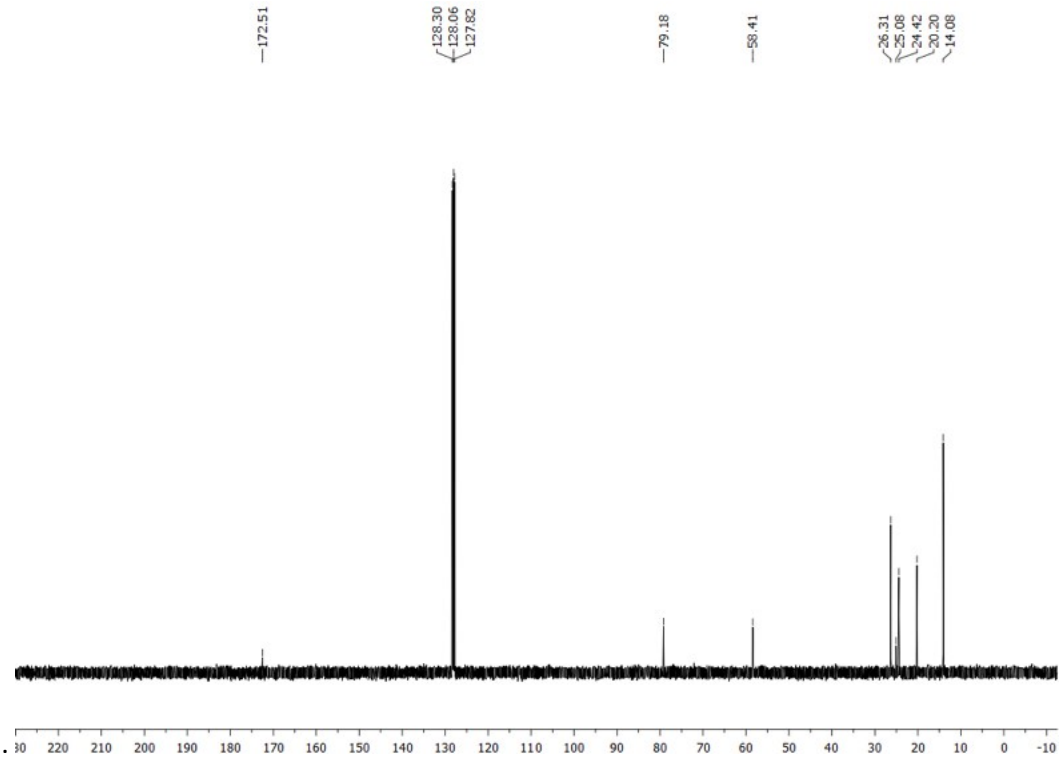

Figure S30. ^{13}C NMR spectrum (C_6D_6) after the stoichiometric reaction between [TBA][OAc] and HBpin (1h, RT).

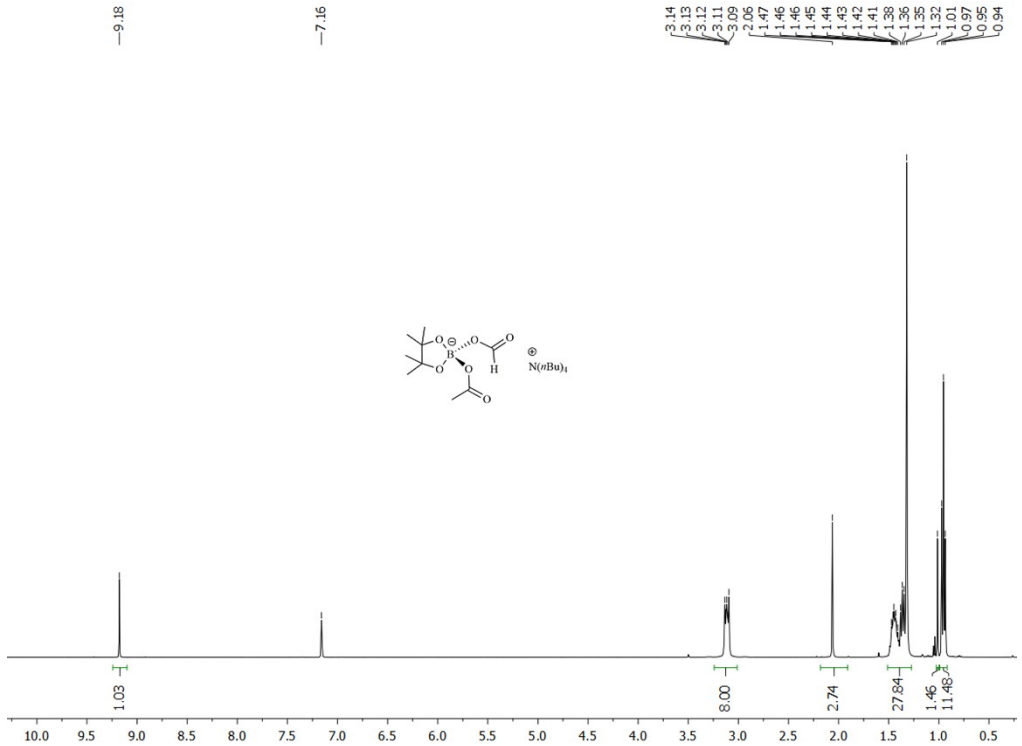

Figure S31. ^{1}H NMR spectrum (C_6D_6) of the reaction mixture after exposing a 1/1 [TBA][OAc] and HBpin under 1.5 atm of CO_2, consistent with the complete formation of the CO_2 insertion product $[pinB(OAc)(O_2CH)]^-$ (**4**).

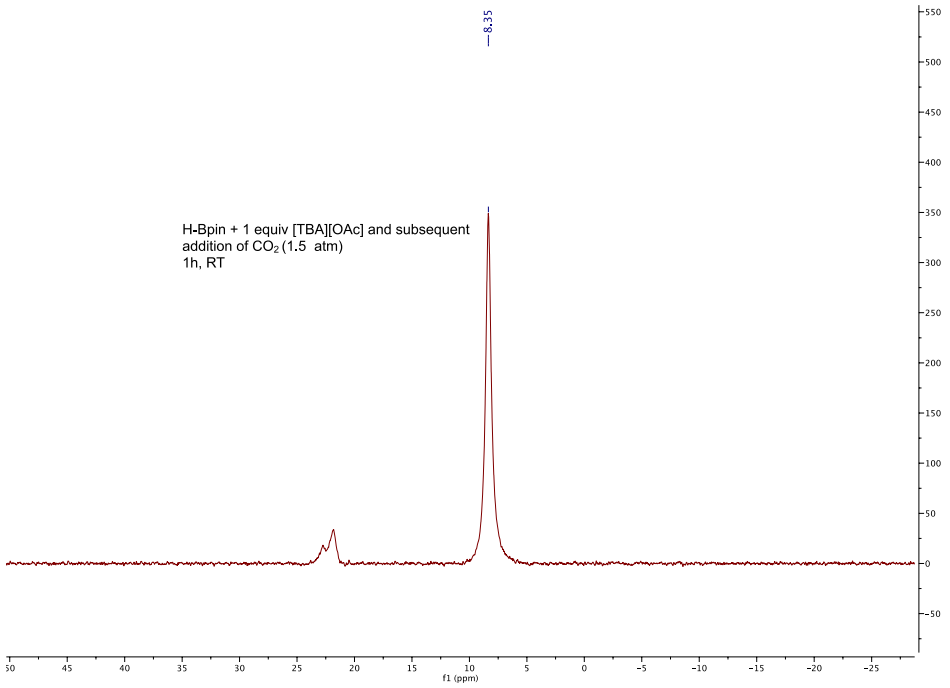

Figure S32. ^{1}H NMR spectrum (C_6D_6) of the reaction mixture after exposing a 1/1 [TBA][OAc] and HBpin under 1.5 atm of CO_2, consistent with the complete formation of the CO_2 insertion product $[pinB(OAc)(O_2CH)]^-$ (**4**).

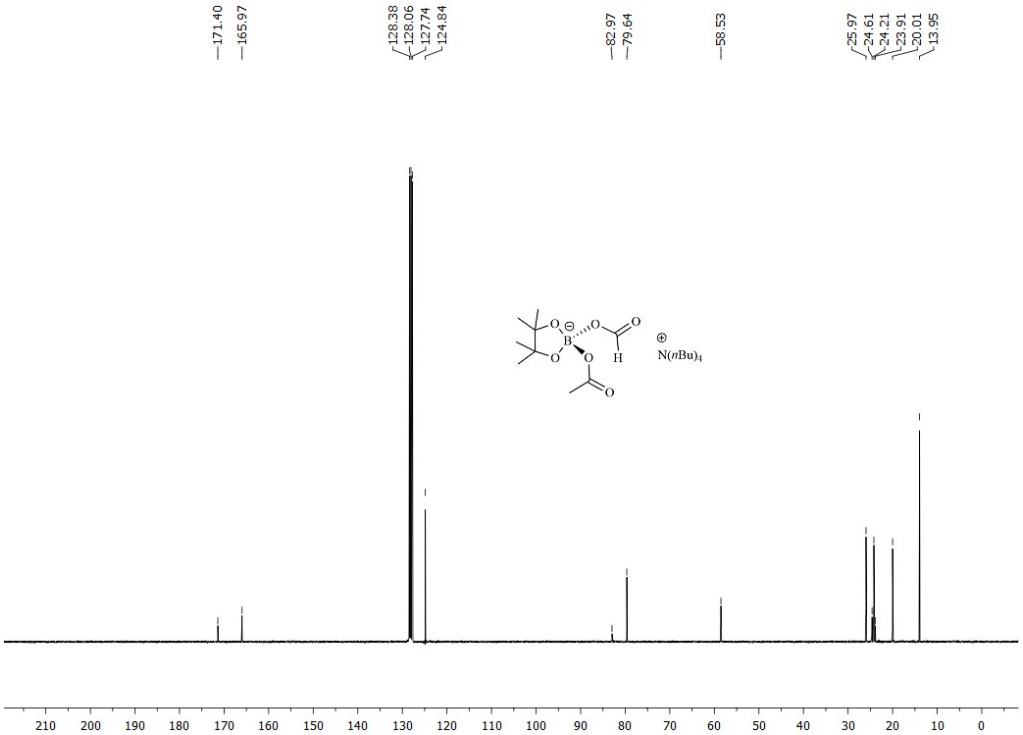

Figure S33. ^{13}C NMR spectrum (C_6D_6) of the reaction mixture after exposing a 1/1 [TBA][OAc] and HBpin under 1.5 atm of CO_2, consistent with the complete formation of the CO_2 insertion product $[pinB(OAc)(O_2CH)]^-$ (**4**).

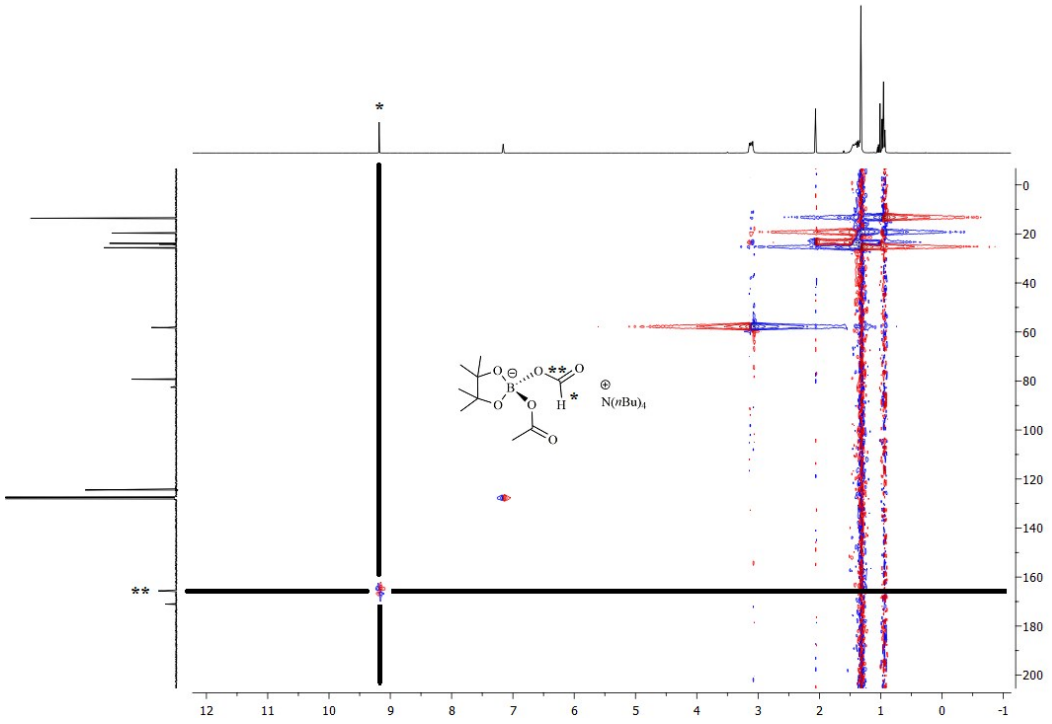

Figure S34. 2D HSQC NMR spectrum (C_6D_6) of the reaction mixture after exposing a 1/1 [TBA][OAc] and HBpin under 1.5 atm of CO_2, consistent with the complete formation of the CO_2 insertion product $[pinB(OAc)(O_2CH)]^-$ (**4**).

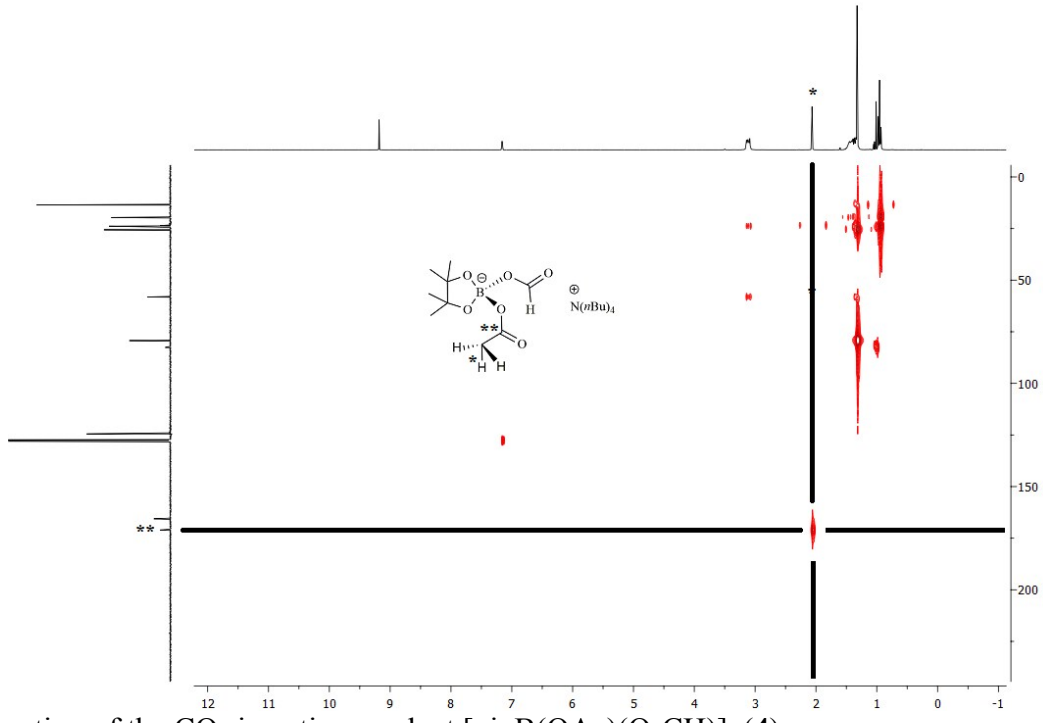

Figure S35. 2D HMBC NMR spectrum (C_6D_6) of the reaction mixture after exposing a 1/1 [TBA][OAc] and HBpin under 1.5 atm of CO_2, consistent with the complete formation of the CO_2 insertion product $[pinB(OAc)(O_2CH)]^-$ (**4**).

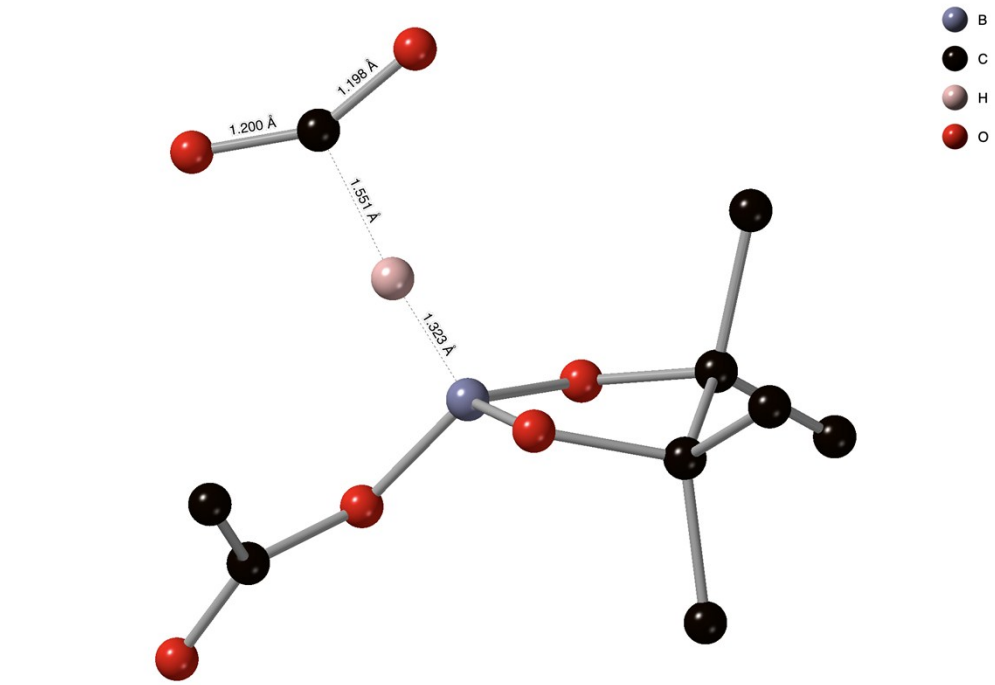

Figure S36. Molecular structure of **TS-1** as estimated by DFT calculations (wB97xD/def2tzvpp//B3LYP/6-31G*)

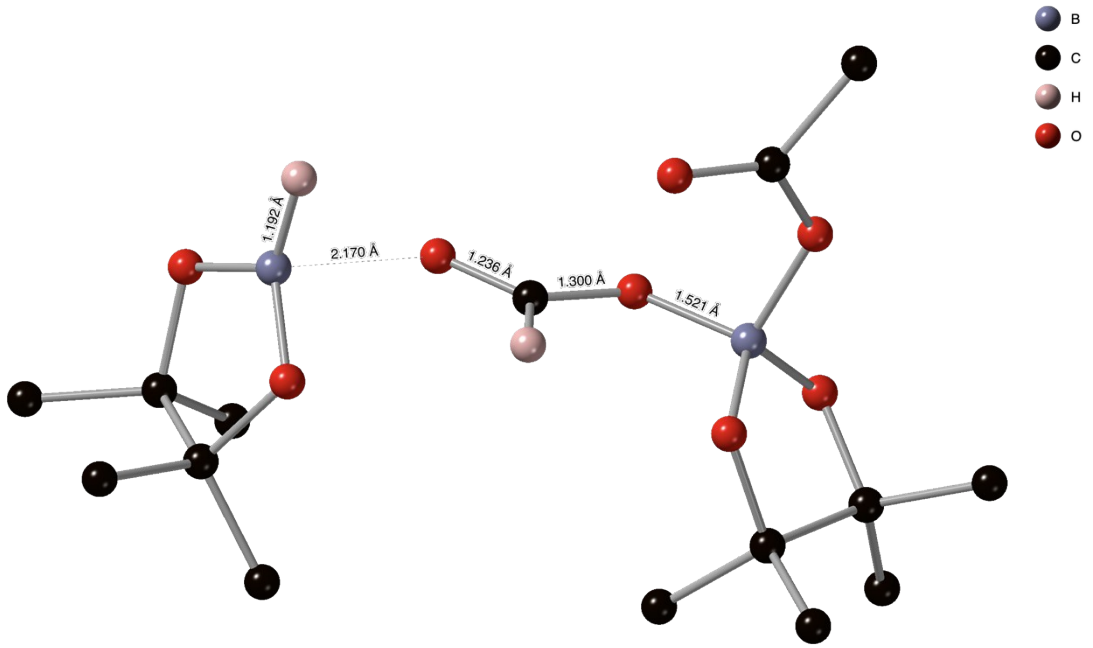

Figure S37. Molecular structure of **TS-2** as estimated by DFT calculations (wB97xD/def2tzvpp//B3LYP/6-31G*)

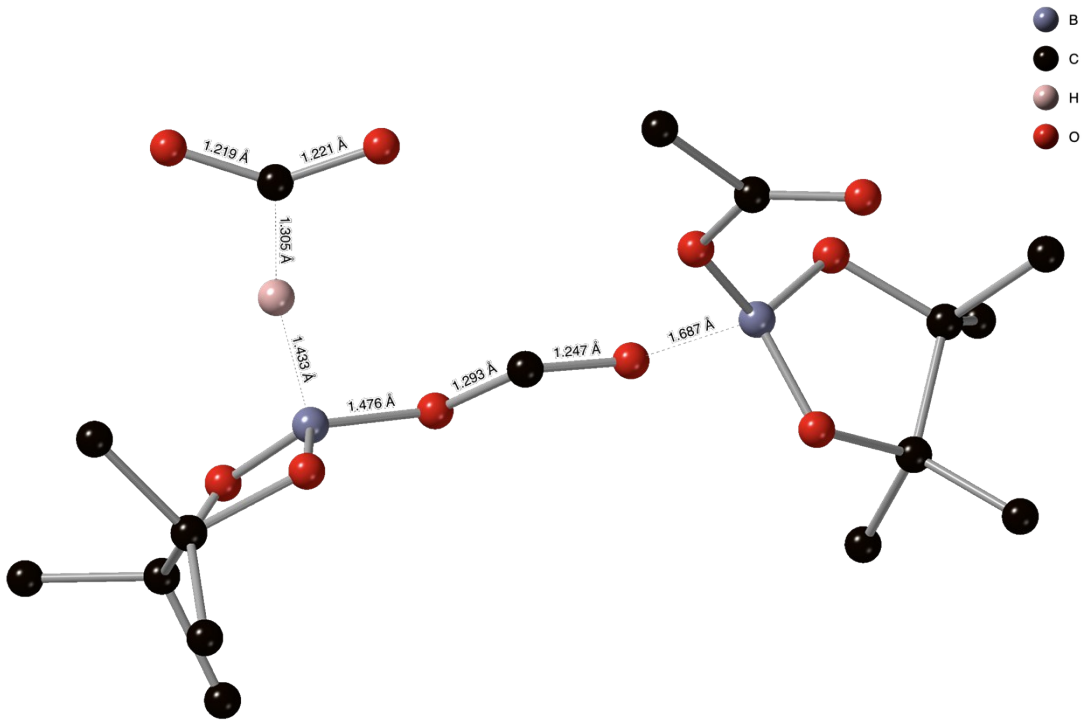

Figure S38. Molecular structure of **TS-3** as estimated by DFT calculations (wB97xD/def2tzvpp//B3LYP/6-31G*)

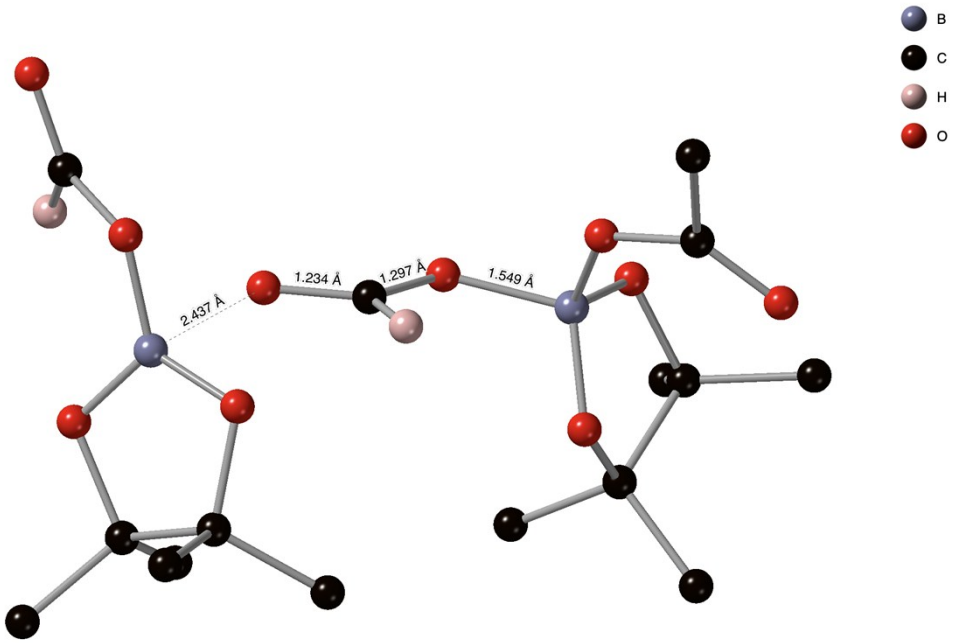

Figure S39. Molecular structure of **TS-4** as estimated by DFT calculations (wB97xD/def2tzvpp//B3LYP/6-31G*)

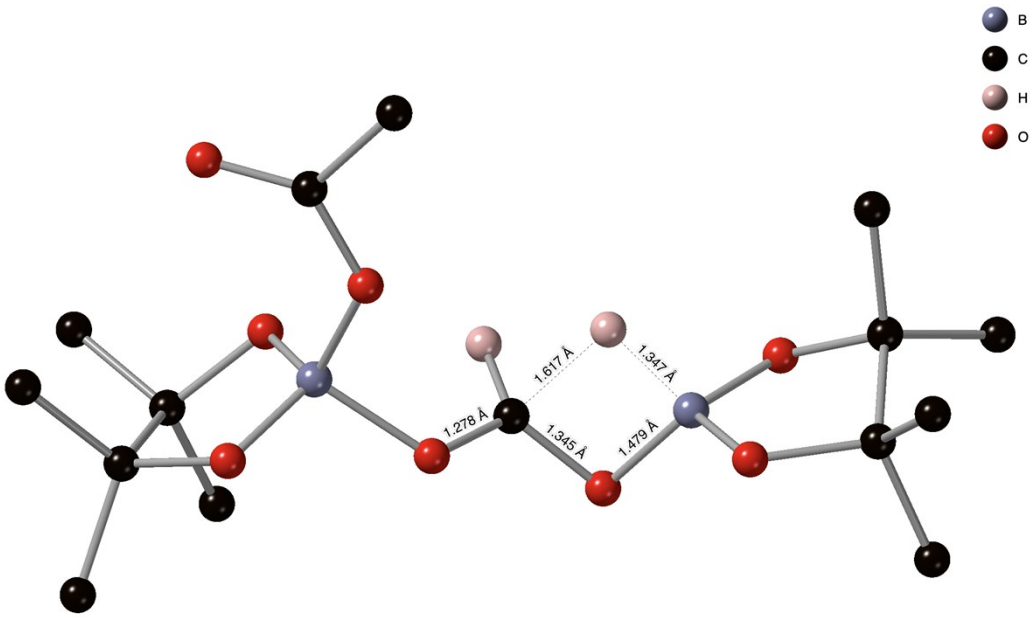

Figure S40. Molecular structure of **TS-5** as estimated by DFT calculations (wB97xD/def2tzvpp//B3LYP/6-31G*)

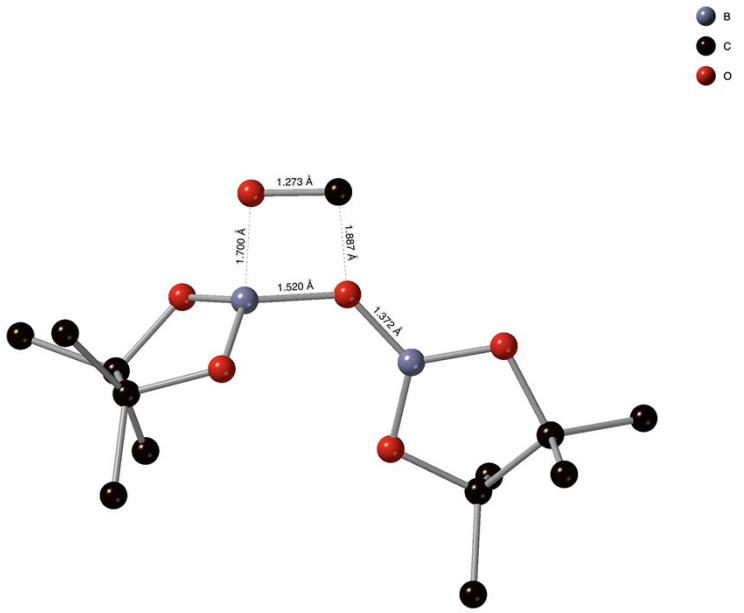

Figure S41. Molecular structure of **TS-6** as estimated by DFT calculations (wB97xD/def2tzvpp//B3LYP/6-31G*)

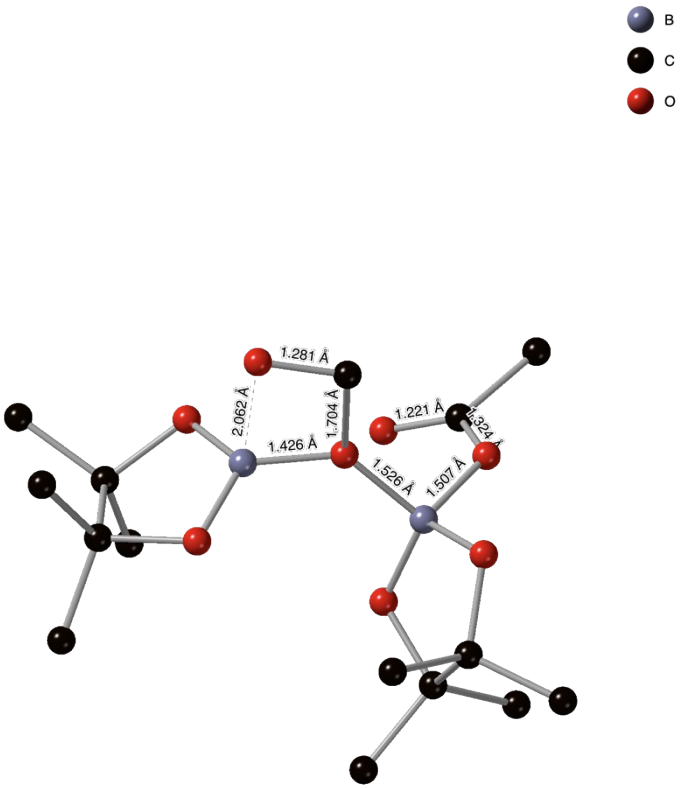

Figure S42. Molecular structure of **TS-7** as estimated by DFT calculations (wB97xD/def2tzvpp//B3LYP/6-31G*)

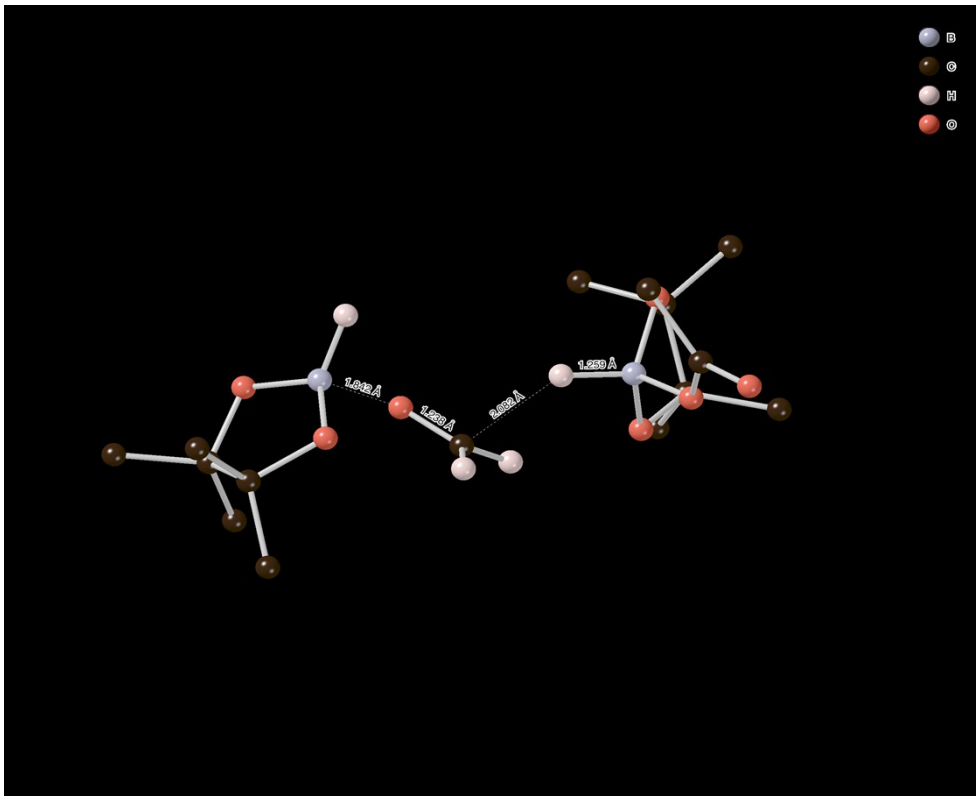

Figure S43. Molecular structure of **TS-8** as estimated by DFT calculations (wB97xD/def2tzvpp//B3LYP/6-31G*)

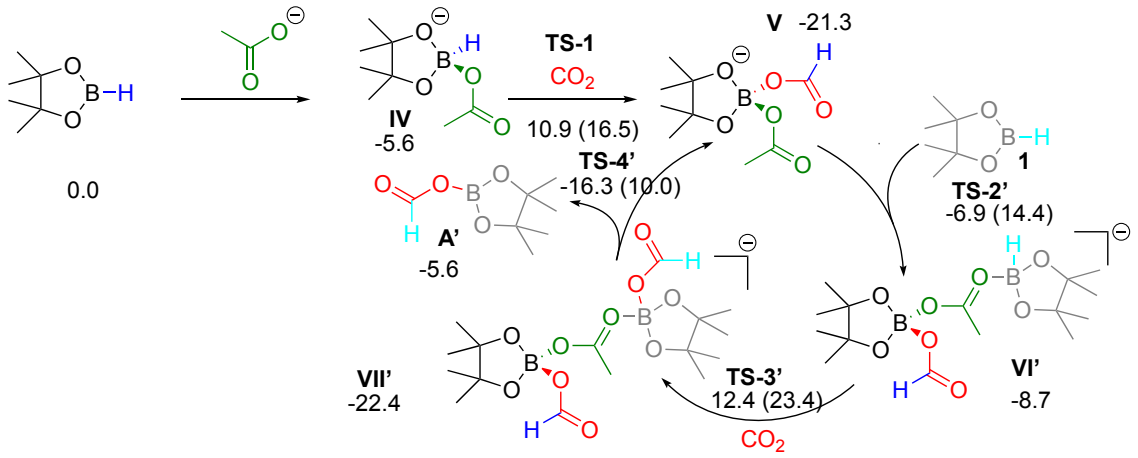

Figure S44. DFT-estimated mechanism (wB97xD/def2tzvpp//B3LYP/6-31G*, benzene) of acetate-catalyzed CO_2 hydroboration to model **A'** through the formation of acetate-bridged dinuclear boron model **VI'**. The values in parenthesis correspond to the energy barriers.